Iranian Journal of
Numerical Analysis and Optimization

Ferdowsi University of Mashhad

Reaserch Article

Memory-driven fractional dynamics of pneumonia transmission with prophylactic intervention

K. Soni, S. Kumar, S. Kumawat and A.K. Sinha

DOI:10.22067/ijnao.2026.97941.1852

Vol. 17, No. 1, March 2027

pp. 290–331

Ferdowsi University of Mashhad, Iran

Iranian Journal of Numerical Analysis and Optimization
Vol. 17, No. 1, 2027, pp 290–331
https://doi.org/10.22067/ijnao.2026.97941.1852
https://ijnao.um.ac.ir/

CC BY NC

Research Article

Memory-driven fractional dynamics of pneumonia transmission with prophylactic intervention

K. Soni, S. Kumar, S. Kumawat and A.K. Sinha*

Abstract

A novel fractional-order mathematical model is proposed to investigate the transmission dynamics of Pneumocystis pneumonia in an immunocompromised population. Long-term chemoprophylaxis is represented as an imperfect vaccination strategy within a susceptible-vaccinated-infected framework. The model is formulated using the Atangana–Baleanu fractional derivative in the Caputo sense to incorporate memory and hereditary effects in disease transmission. The positivity, boundedness, existence, uniqueness, and Ulam–Hyers stability of the proposed system are established. The basic reproduction number ($\mathfrak{R}_0$) is derived using the next-generation

*Corresponding author

Received 19 February 2026; revised 14 July 2026; accepted 25 July 2026

Kaushal Soni
Department of Mathematics, National Institute of Technology Raipur, India. e-mail: kaushalmath2205@gmail.com

Sanjeev Kumar
Department of Mathematics, Khandari Campus, Agra India. Maharaja Suhel Dev University Azamgarh India. e-mail: sanjeevibs@yahoo.co.in

Shyamsunder Kumawat
Department of Mathematics, SRM University Delhi-NCR, Sonepat, Haryana, India. e-mail: skumawatmath@gmail.com

Arvind Kumar Sinha
Department of Mathematics, National Institute of Technology Raipur, India. e-mail: aksinha.maths@nitrr.ac.in

How to cite this article
Soni, K., Kumar,S., Kumawat, S. and Sinha, A.K., Memory-driven fractional dynamics of pneumonia transmission with prophylactic intervention. *Iran. J. Numer. Anal. Optim.*, 2027; 17(1): 290-331. https://doi.org/10.22067/ijnao.2026.97941.1852

matrix approach, and the local asymptotic stability of the disease-free and endemic equilibrium points is investigated. A numerical scheme based on Lagrange interpolation is employed to obtain approximate solutions. Sensitivity analysis is performed to identify the parameters that most strongly influence disease transmission. The results indicate that increasing prophylaxis coverage and efficacy substantially reduces the basic reproduction number and suppresses disease spread. The proposed fractional-order framework provides a realistic description of pneumonia dynamics by incorporating memory effects and offers useful insights for evaluating prophylactic intervention strategies in vulnerable populations.

AMS subject classifications (2020): 26A33; 34A08; 34D20; 34K20; 37N25.

Keywords: Pneumonia transmission; Fractional-order model; Prophylaxis; Imperfect vaccine; Mathematical epidemiology; Stability analysis.

1 Introduction

Pneumonia is still one of the most serious health problems worldwide and is responsible for more than 700,000 children under 5 years dying each year, which is about one child every 43 seconds. It is also the top infectious cause of death among children globally [57]. The damage does not stop with children; in fact, last year, pneumonia led to more than one million deaths among people over 70 years of age, thus reflecting its heavy toll on people of all ages [51]. Pneumocystis pneumonia, caused by the fungal pathogen Pneumocystis jirovecii, is one of the serious complications of immunodeficiency and, therefore, a distinguishing infection with a growing threat. While originally it was one of the AIDS epidemic's hallmark diseases, Pneumocystis pneumonia has been increasingly detected in non-HIV immunocompromised patients. Thus, it can be very well seen in the cases of organ transplant recipients, people with cancer who undergo chemotherapy, and patients who are on long-term immunosuppressive treatment

[31, 27, 58, 12, 16]. The death toll of Pneumocystis pneumonia in non-HIV-infected individuals is alarmingly high, as it is reported to be between 30% and 50%, whereas in HIV-positive cases, it accounts for only $10 - 20\%$ [36, 19]. The major route of transmission is through the air, thereby spreading the disease from one person to another and leading to hospital-based outbreaks (nosocomial), notably in transplant units, where such outbreaks have been well documented. These outbreaks demonstrate the necessity of implementing infection prevention and control measures strictly [25, 60, 4]. Given its extremely high fatality rate and easy spread, clinical management is mainly characterised by the use of long-term chemoprophylaxis and early detection using advanced molecular diagnostic tools [50, 18, 8, 35]. Many theoretical approaches

have been developed to better understand the complex epidemiological dynamics of Pneumocystis pneumonia. Different mathematical modeling approaches have been employed to explore transmission mechanisms, study co-infection dynamics, evaluate the effects of interventions and fractional-order calculus [56, 55].

Mathematical models play a crucial role in analyzing how pneumonia spreads through populations and in developing interventions to reduce its prevalence. Several mathematical models employing integer-order derivatives have been constructed to analyze disease dynamics [45, 17, 13, 2]. Several key studies have focused on pneumonia transmission, including Manuputty, Lesnussa, and Leleury [26] witch investigated the stability and the impact of vaccination. Osiuigbo et al. [29] developed a model to study the dissemination of pneumonia. Kizito and Tumwiine [21] examined the combined impact of vaccination and treatment in controlling pneumococcal pneumonia. Kanyiri, Luboobi, and Kimathi [20] analyzed optimal strategies for controlling co-infection of influenza and pneumonia, taking into account the development of antiviral resistance. Teklu [54] examined the spread and transmission patterns of HIV/AIDS and pneumonia co-infection.

For a complex infection like Pneumocystis pneumonia, where transmission occurs within a specific, vulnerable subpopulation and preventative medication (prophylaxis) is a key intervention, mathematical modeling offers a unique opportunity to quantify the effects of prophylaxis coverage and efficacy on disease control. The application of mathematical modeling to pneumonia has yielded a growing body of literature aimed at understanding its transmission and control and several studies have employed integer-order differential equation models to explore intervention strategies.

Although studies [26, 29, 21, 20, 54] have significantly improved the understanding of pneumonia transmission, they mainly rely on classical integer-order differential equation models and investigate bacterial pneumonia, coinfection, vaccination, treatment, or optimal control strategies. None of these studies considers Pneumocystis pneumonia as a standalone disease in an immunocompromised population, nor do they model long-term chemoprophylaxis as an imperfect vaccination strategy. Furthermore, the existing models do not incorporate the Atangana–Baleanu fractional derivative with a nonsingular and nonlocal kernel, which enables the inclusion of memory and hereditary effects that are important for describing chronic disease progression and long-term prophylactic interventions. In addition, the proposed model establishes the positivity, boundedness, existence, uniqueness, Ulam–Hyers (UH) stability, equilibrium analysis, sensitivity analysis, and numerical simulations within a unified fractional-order framework. These features clearly distinguish the proposed model from the previously published studies. Therefore, the main novelty of the present work lies in the development of the first fractional-order susceptible-vaccinated-infected model for Pneumocystis pneumonia using the Atangana–Baleanu fractional derivative. Unlike previous studies, the proposed model treats chemoprophylaxis as an imperfect

vaccination strategy, explicitly incorporates memory effects through a nonsingular and nonlocal kernel, and provides a comprehensive theoretical and numerical analysis for assessing the impact of prophylaxis coverage and efficacy on disease transmission.

Several fractional operators utilizing power-law, exponential, generalized Mittag-Leffler (ML), and other kernel functions have been introduced, gaining notable interest in the modeling of biological processes [10, 11, 3]. Fractional-order operators offer advantages over classical-order operators, including memory effects and improved performance. Fractional-order operators have been successfully applied to Marburg virus, COVID-19, Hepatitis B, Zika virus, and Malaria disease modeling to investigate their spread and control [46, 5, 48, 47, 42, 37, 41, 49, 44, 38, 24, 43]. Specifically, Sabar et al. [33] examined strategies for managing pneumonia in livestock. Peter et al. [30] developed and studied a pneumococcal pneumonia model incorporating the Caputo–Fabrizio operator. They conducted numerical simulations and assessed the role of arbitrary fractional-order derivatives using model parameters, concluding that the force of infection plays a crucial role in controlling disease spread within a community.

Fractional-order differential equations offer a more precise modeling approach for real-world systems than conventional integer-order models [6, 59, 7, 23, 22]. Several fractional derivatives have been defined, broadening the classical integer-order derivative. Riemann and Liouville [34] laid the groundwork with their definition of the classical fractional-order derivative. One example of its application is the study of nematic liquid crystal diffusion using the fractional Hunter–Saxton equation [14]. Caputo and Fabrizio [11] introduced a fractional-order derivative characterized by an exponential kernel, further examined in [15, 32]. Subsequently, Atangana and Baleanu [3] proposed a fractional operator incorporating the ML function as its kernel, which possesses nonsingular and nonlocal properties. Unlike the Caputo–Fabrizio derivative, which uses a nonsingular exponential kernel, the Atangana–Baleanu fractional derivative in the Caputo sense employs a nonsingular and nonlocal Mittag-Leffler kernel. Hence, the Atangana–Baleanu fractional derivative in the Caputo sense is better suited to capture the long-term memory and hereditary effects involved in Pneumocystis pneumonia transmission.

While traditional integer-order epidemic models effectively describe local dynamics in the absence of external factors, they fail to capture the nonlocal interactions and crossover effects observed in many biological systems. Classical fractional-order operators, constrained by their singular kernels, also struggle to represent these complexities accurately. In contrast, the Atangana–Baleanu fractional derivative in the Caputo sense, with its generalized ML kernel, excels in modeling such intricate behaviors, including crossover effects in mean-square displacement. Additionally, its nonsingular kernel enhances the accuracy of predictions regarding both the early and late stages of disease transmission.

To date, no study has applied the sophisticated framework of fractional-order modeling to investigate the transmission dynamics of Pneumocystis Pneumonia as a standalone infection within its specific at-risk, immunocompromised population. Furthermore, the critical public health strategy of long-term chemoprophylaxis in this group has never been conceptually modeled as a form of "vaccination" within a fractional susceptible-vaccinated-infected framework with the Atangana–Baleanu fractional derivative in the Caputo sense. Therefore, our proposed study is uniquely positioned to bridge this gap by taking advantage of the methodological advantages of fractional calculus to analyze the specific epidemiology and the novel Pneumocystis pneumonia control paradigm.

Thus, to clearly address the identified gap in the present literature, this research project aims to develop and conduct a thorough analysis of a novel fractional-order susceptible-vaccinated-infected epidemiological model tailored to the transmission dynamics of Pneumocystis pneumonia. Firstly, one of the significant innovations of this article is to be among the handful of studies that have utilized a fractional-order modeling method in the particular epidemiological framework of Pneumocystis pneumonia. Through the Atangana–Baleanu fractional derivative in Caputo, the model can capture memory and hereditary features, which are essential for representing the nature of chronic infections and the susceptibility cycle of immunocompromised individuals over a long period. Secondly, the study, in a more conceptual and groundbreaking manner, redefines the long-term use of chemoprophylaxis, the main weapon against Pneumocystis pneumonia, as a form of imperfect vaccination within the model. This viewpoint not only provides a new theoretical basis for prophylactic assessment but also enhances understanding of its epidemiological effects at the population level.

This paper is structured in the following manner: Foundational principles of fractional calculus are presented in Section 2. Section 3 details the construction of the proposed mathematical model. The qualitative analysis of the model is the focus of Section 4, followed by an examination of UH stability in Section 5. In Section 6, we determine the basic reproduction number, equilibrium states, and stability analysis. A sensitivity analysis is conducted in Section 7. The numerical scheme implemented for simulations and the findings are discussed in Section 8. Finally, conclusions are drawn, and potential future research avenues are suggested in Section 9.

2 Preliminaries

This section begins with examining fundamental mathematical tools utilized in the following sections.

Definition 1 ([52]). Consider $m \in [1, \infty)$, and let $\mathbb{J}$ be an open subset. Then the Sobolev space $H^m(\mathbb{J})$ is expressed as follows:

$H^m(\mathbb{J}) = \{\mathscr{U} \in L^2(\mathbb{J}) \big| \mathcal{D}^{\xi}\mathscr{U} \in L^2(\mathbb{J}) \ \forall |\xi| \leq m\}.$

Atangana and Baleanu [3] formulated the Atangana–Baleanu fractional derivative in Caputo sense using this definition.

Definition 2 ([3]). Consider a function $\mathscr{G}(t) \in H^m(c, d)$, and let ξ be a fractional order such that $0 < \xi < 1$. Then, the Atangana–Baleanu fractional derivative in the Caputo sense is expressed as follows:

$$ {}^{ABC}_{\ \ 0}D^{\xi}_{t}\mathscr{G}(t) = \frac{ABC(\xi)}{(1-\xi)} \int_0^t E_{\xi}\left(\frac{-\xi}{1-\xi}(t-\varrho)^{\xi}\right)\mathscr{G}' d\varrho, \tag{1} $$

where $ABC(\xi)$ is a normalization mapping such that $ABC(0) = ABC(1) = 1$.

Definition 3 ([3]). The Laplace transform (LT) of the function $\mathscr{G}(t)$ is commonly defined as follows:

$$ \mathscr{L}[\mathscr{G}(t), s] = \overline{\mathscr{G}}(s) = \int_0^{\infty} e^{-st}\mathscr{G}(t)dt, \qquad \mathbb{R}(s) > \zeta, \quad t \geq 0. \tag{2} $$

Taking inverse LT of $\overline{\mathscr{G}}(s)$, we have

$$ \mathscr{L}^{-1}[\overline{\mathscr{G}}(s), t] = \frac{1}{2\pi i}\int_{\eta - i\infty}^{\eta + i\infty} e^{st}\overline{\mathscr{G}}(s)ds, \text{where} \ \ \eta \in \mathbb{R}. \tag{3} $$

Definition 4 ([3]). The LT of Atangana–Baleanu fractional derivative in the Caputo sense is expressed as follows:

$$ \mathscr{L}\left[{}^{ABC}_{\ \ 0}D^{\xi}_{t}\mathscr{G}(t)\right] = \frac{ABC(\xi)}{1-\xi}\left[\frac{s^{\xi}\mathscr{L}\{\mathscr{G}(t)\} - s^{\xi-1}\mathscr{G}(0)}{s^{\xi} + \frac{\xi}{1-\xi}}\right]. \tag{4} $$

Definition 5 ([3]). Let $\mathscr{G}(t) \in H^m(a, b)$, and consider a fractional order ξ with $0 < \xi < 1$ then the fractional integral in the Atangana–Baleanu sense is defined as follows:

$$ {}^{ABC}_{\ \ 0}\mathfrak{I}^{\xi}_{t}\mathscr{G}(t) = \frac{1-\xi}{ABC(\xi)}\mathscr{G}(t) + \frac{\xi}{ABC(\xi)\Gamma(\xi)}\int_0^t (t-\tau)^{\xi-1}\mathscr{G}(\tau)d\tau. \tag{5} $$

Definition 6. For $\Psi > 0$, the Mittag-Leffler function $E_\Psi(\mathfrak{z})$ was first proposed by Mittag-Leffler, while its two-parameter generalization, $E_{\Psi,\varpi}(\mathfrak{z})$, is credited to Wiman,

$$E_\Psi(\mathfrak{z}) = \sum_{n=0}^{\infty} \frac{\mathfrak{z}^k}{\Gamma(\Psi k + 1)} \qquad (\mathfrak{z}, \Psi \in \mathbb{C}, \mathbb{R}(\Psi) > 0), \tag{6}$$

$$E_{\Psi,\varpi}(\mathfrak{z}) = \sum_{n=0}^{\infty} \frac{\mathfrak{z}^k}{\Gamma(\Psi k + \varpi)}, \qquad (\mathfrak{z}, \Psi, \varpi \in \mathbb{C}, \mathbb{R}(\Psi) > 0, \mathbb{R}(\varpi) > 0). \tag{7}$$

Lemma 1 ([39])**.** For $0 < \xi \leq 1$, we consider the fractional differential problem described as follows:

$${}^{ABC}_{\ \ 0}D_t^{\xi}\mathscr{G}(t) = \mathscr{B}(t), \qquad t \in [0, T], \quad \mathscr{G}(0) = \mathscr{G}_0, \tag{8}$$

where $\mathscr{G} : [0, T] \to \mathbb{R}$ is a function and $\mathscr{G}_0$ is a fixed point such that

$$\mathscr{G}(t) = \mathscr{G}_0 + \frac{1-\xi}{ABC(\xi)}\mathscr{B}(t) + \frac{\xi}{ABC(\xi)\Gamma(\xi)}\int_0^t (t-\tau)^{\xi-1}\mathscr{B}(\tau)d\tau. \tag{9}$$

Lemma 2. Let $\phi : D \to \mathbb{R}^n$ with $\phi \in C^1(D)$ and let $x \in D \subseteq \mathbb{R}$. Then ϕ fulfills a Lipschitz condition on each convex compact set $D \subseteq D$ with Lipschitz constant $\mathbb{K} > 0$ such that

$$\mathbb{K} = \max_{x \in D}\left|\frac{d\phi}{dx}\right|.$$

Lemma 3. Let $\mathcal{F}(t) \in C[a, b]$, and assume its Atangana–Baleanu fractional derivative ${}^{ABC}_{\ \ 0}D_t^{\xi}\mathcal{F}(t) \in C[a, b]$ for $0 < \xi \leq 1$. Then, for every $t \in [a, b]$ there exists a point $l_1 \in [a, t]$ such that

$$\mathcal{F}(t) - \mathcal{F}(a) = \left[1 - E_\xi\left(-\frac{\xi(t-c_1)^\xi}{1-\xi}\right)\right]^{-1} \frac{(t-a)^\xi}{ABC(\xi)\Gamma(\xi)}\ {}^{ABC}_{\ \ 0}D_t^{\xi}\mathcal{F}(l_1), \tag{10}$$

where $c_1 \in (a, t)$.

Lemma 4 (Generalized mean value theorem [28])**.** Let $g(t) \in C[a, b]$, and let ${}^{ABC}_{\ \ 0}D_t^{\xi}g(t) \in C[a, b]$ when $0 < \xi \leq 1$ Then $g(t) = g(a) + \frac{1}{\Gamma(\xi)}\ {}^{ABC}_{\ \ 0}D_t^{\xi}g(\delta)(t-a)^\xi$, when $0 \leq \delta \leq t$, for all $t \in (a, b]$

Note that by Lemma 4 if $g(t) \in (0,b]$, and ${}^{ABC}_{0}D^{\xi}_{t}g(t) \in C(a,b]$ ${}^{ABC}_{0}D^{\xi}_{t}g(t) \leq 0$ for every $t \in (0,b]$, the function $g(t)$ is nonincreasing on for all $t \in (0,b]$ and ${}^{ABC}_{0}D^{\xi}_{t}gF(t) \geq 0$ for every $t \in (0,b]$, then the function $g(t)$ is nondecreasing for all t in $(0,b]$.

Theorem 1 (Schaefer's fixed point theorem [9])**.** Let V be a normed linear space, and let T be a continuous mapping of V into V that is compact on each bounded subset X of V. Then set $W = \left\{x \in V : \ x = \lambda T(x) \text{ for some } 0 \leq \lambda \leq 1\right\}$ is bounded. Then T has a fixed point.

3 Model formulation

To investigate the transmission dynamics of Pneumocystis Pneumonia, a serious fungal infection, we propose a compartmental model based on its modern epidemiological understanding. Caused by the fungus Pneumocystis jirovecii, Pneumocystis Pneumonia is now understood to spread directly from person to person via an airborne route [25]. The disease primarily poses a threat to individuals with compromised immune systems, such as organ transplant recipients, patients undergoing chemotherapy, or those with HIV/AIDS [53, 27]. A key strategy in managing Pneumocystis Pneumonia is the use of long-term chemoprophylaxis (preventative medication) in these at-risk populations [50]. In this study, we innovatively model this public health intervention as a form of vaccination. This allows us to use a susceptible-vaccinated-infected ($\mathcal{XYZ}$) framework to analyze the impact of prophylaxis coverage and efficacy on the spread of the disease. The model is specifically designed to capture the dynamics within the vulnerable, immunocompromised population, where the infection is most prevalent and severe. In this work, the total population $\mathscr{N}$ is partitioned into three mutually exclusive compartments. The class $\mathcal{X}$ denotes immunocompromised individuals who are susceptible to Pneumocystis Pneumonia and are not receiving prophylactic protection. The class $\mathcal{Y}$ represents the population of immunocompromised individuals who are receiving prophylactic treatment. This group is analogous to a vaccinated population, having a significantly reduced, but not zero, probability of infection. The class $\mathcal{Z}$ represents the population of individuals who are actively infected with Pneumocystis Pneumonia and are capable of transmitting the fungus to individuals in both the $\mathcal{X}$ and $\mathcal{Y}$ compartments.

To account for the memory and nonlocal effects associated with the progression and transmission of Pneumocystis Pneumonia, the proposed $\mathcal{XYZ}$ model is formulated using the Atangana–Baleanu fractional derivative in Caputo. The Atangana–Baleanu fractional derivative in Caputo is characterized by a nonsingular kernel, which allows past states of the system to influence the current dynamics in a biologically realistic manner. The governing equations are considered in the Atangana–Baleanu fractional derivative in Caputo sense with order $0 < \xi \leq 1$ as follows:

$$
\begin{aligned}
{}^{ABC}_{\ \ 0}D^{\xi}_{t}\mathcal{X}(t) &= (1-p)\Lambda - \frac{\beta_1\mathcal{X}\mathcal{Z}}{\mathcal{X}+\mathcal{Y}+\mathcal{Z}} - \mu_1\mathcal{X},\\
{}^{ABC}_{\ \ 0}D^{\xi}_{t}\mathcal{Y}(t) &= p\Lambda - \frac{(1-\psi)\beta_2\mathcal{Y}\mathcal{Z}}{\mathcal{X}+\mathcal{Y}+\mathcal{Z}} - \mu_2\mathcal{Y},\\
{}^{ABC}_{\ \ 0}D^{\xi}_{t}\mathcal{Z}(t) &= \frac{\beta_1\mathcal{X}\mathcal{Z}}{\mathcal{X}+\mathcal{Y}+\mathcal{Z}} + \frac{(1-\psi)\beta_2\mathcal{Y}\mathcal{Z}}{\mathcal{X}+\mathcal{Y}+\mathcal{Z}} - \mu_3\mathcal{Z},
\end{aligned}
\tag{11}
$$

with initial conditions $\mathfrak{P}_0 = (\mathcal{X}_0, \mathcal{Y}_0, \mathcal{Z}_0)$ and total population size $\mathscr{N} = \mathcal{X}+\mathcal{Y}+\mathcal{Z}$.

The formulation of our model rests on the following key assumptions about Pneumocystis Pneumonia. Transmission mechanism: Infection occurs through airborne exposure, whereby individuals in the infected class ($\mathcal{Z}$) transmit the fungus to both susceptible ($\mathcal{X}$) and prophylaxis-protected ($\mathcal{Y}$) individuals. The resulting infection pressure is described using a standard incidence function. Target population: The model focuses solely on the vulnerable, immunocompromised population. The recruitment parameter Λ denotes the rate at which individuals newly enter this at-risk group, such as through organ transplantation, initiation of immunosuppressive treatment, or new HIV diagnoses. Prophylactic intervention: Upon entry into the at-risk population, a proportion p of individuals is assumed to immediately initiate chemoprophylaxis and therefore join the protected class $\mathcal{Y}$, while the remaining fraction $(1-p)$ enters the susceptible class $\mathcal{X}$ Imperfect protection: Prophylactic treatment is assumed to provide partial protection. With efficacy level ψ, individuals in the protected class $\mathcal{Y}$ remain susceptible to infection, though their risk is reduced by a factor of $(1-\psi)$.

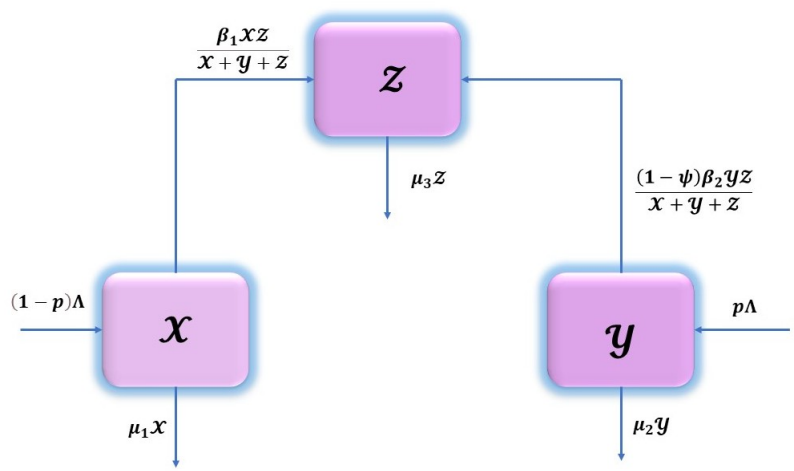

Figure 1: Schematic diagram for the Pneumonia transmission.

According to the model description and the parameters in Table 1, the schematic diagram is represented by Figure 1 below.

Table 1: Description of parameters in model (11).

Parameters	Description	value	Source
Λ	Recruitment rate of susceptible immunocompromised individuals	10.9	[21]
β_1	Transmission rate from infected to unprotected susceptibles	0.0287	[21]
β_2	Transmission rate from infected to prophylaxis-protected	0.0286	Assumed
μ_1	Natural mortality rate of susceptible individuals without protection	0.0002	[1]
μ_2	Natural Mortality rate of prophylaxis-protected individuals	0.0001	Fitted
μ_3	Total Mortality rate of infected individuals	0.3302	[1]
ψ	Efficacy of the prophylactic drug regimen	[0,1]	Assumed
p	Coverage rate of prophylaxis among new at-risk individuals	[0,1]	Assumed

4 Qualitative analysis

This section provides a mathematical analysis of solution behavior, such as positivity, existence, uniqueness, and boundedness.

4.1 Positivity and boundedness

This part focuses on proving that,given all initial state variables are positive,the model consistently yields solutions that are not only finite but also stay nonnegative for every $t > 0$. The proof relies on the application of the subsequent theorem.

Theorem 2. The proposed infection system (11) provides positive and bounded solutions for positive initial conditions.

Proof. We first prove that every solution $(\mathcal{X}(t), \mathcal{Y}(t), \mathcal{Z}(t))$ of system (11) is nonnegative for all $t > 0$; that is, $\mathcal{X}(t), \mathcal{Y}(t)$, and $\mathcal{Z}(t)$ remain greater than or equal to zero.
To show that the set

$$\Omega = \left\{ (\mathcal{X}, \mathcal{Y}, \mathcal{Z}) : 0 \leq \mathcal{X} + \mathcal{Y} + \mathcal{Z} \leq \frac{\Lambda}{\mu_1 + \mu_2 + \mu_3} \right\}. \tag{12}$$

is positively invariant, using Lemma 4

$$\begin{cases} {}^{ABC}_{\ \ 0}D^{\xi}_{t}\mathcal{X}(t)\Big|_{\mathcal{X}(t')=0} &= (1-p)\Lambda \geq 0, \\ {}^{ABC}_{\ \ 0}D^{\xi}_{t}\mathcal{Y}(t)\Big|_{\mathcal{Y}(t')=0} &= p\Lambda \geq 0, \\ {}^{ABC}_{\ \ 0}D^{\xi}_{t}\mathcal{Z}(t)\Big|_{\mathcal{Z}(t')=0} &= 0 \geq 0. \end{cases} \tag{13}$$

It follows from (13) that each of the solutions of (11) is nonnegative and remains in $\mathbb{R}^3_+$, and hence the set Ω defined in (12) is positively invariant for model (11). Next, we introduce the total population $\mathscr{N}(t) = \mathcal{X}(t) + \mathcal{Y}(t) + \mathcal{Z}(t)$, then

$$\begin{aligned} {}^{ABC}_{\ \ 0}D^{\xi}_{t}\mathscr{N}(t) &= {}^{ABC}_{\ \ 0}D^{\xi}_{t}\mathcal{X}(t) + {}^{ABC}_{\ \ 0}D^{\xi}_{t}\mathcal{Y}(t) + {}^{ABC}_{\ \ 0}D^{\xi}_{t}\mathcal{Z}(t), \\ {}^{ABC}_{\ \ 0}D^{\xi}_{t}\mathscr{N}(t) &= \Lambda - \mu_1\mathcal{X}(t) + \mu_2\mathcal{Y}(t) + \mu_3\mathcal{Z}(t), \\ {}^{ABC}_{\ \ 0}D^{\xi}_{t}\mathscr{N}(t) &\leq \Lambda - (\mu_1+\mu_2+\mu_3)\mathscr{N}(t), \\ \mathscr{N}(t) &\leq \left(\frac{ABC(\xi)}{ABC(\xi)+(1-\xi)(\mu_1+\mu_2+\mu_3)}\mathscr{N}(0) \right. \\ &\quad \left. + \frac{(1-\xi)\Lambda}{ABC(\xi)+(1-\xi)(\mu_1+\mu_2+\mu_3)}\right) \\ &\quad E_{\xi,1}\left(-\frac{\xi(\mu_1+\mu_2+\mu_3)}{ABC(\xi)+(1-\xi)(\mu_1+\mu_2+\mu_3)}t^{\xi}\right) \\ &\quad + \frac{\xi\Lambda}{ABC(\xi)+(1-\xi)(\mu_1+\mu_2+\mu_3)}E_{\xi,\xi+1} \\ &\quad \left(-\frac{\xi(\mu_1+\mu_2+\mu_3)}{ABC(\xi)+(1-\xi)(\mu_1+\mu_2+\mu_3)}t^{\xi}\right) \\ &\to \frac{\Lambda}{\mu_1+\mu_2+\mu_3} \text{ as } t\to\infty. \end{aligned}$$

Hence (12) is the biologically feasible region of model (11). □

4.2 Existence results

This section focuses on analyzing the qualitative dynamics of the system (11). We begin by introducing

$$\begin{cases} {}^{ABC}_{\ \ 0}D^{\xi}_{t}\mathcal{X}(t) = \aleph_1(t,\mathcal{X},\mathcal{Y},\mathcal{Z}), \\ {}^{ABC}_{\ \ 0}D^{\xi}_{t}\mathcal{Y}(t) = \aleph_2(t,\mathcal{X},\mathcal{Y},\mathcal{Z}), \\ {}^{ABC}_{\ \ 0}D^{\xi}_{t}\mathcal{Z}(t) = \aleph_3(t,\mathcal{X},\mathcal{Y},\mathcal{Z}), \end{cases} \tag{14}$$

where

$$\begin{cases} \aleph_1(t,\mathcal{X},\mathcal{Y},\mathcal{Z}) = (1-p)\Lambda - \frac{\beta_1\mathcal{X}\mathcal{Z}}{\mathcal{X}+\mathcal{Y}+\mathcal{Z}} - \mu_1\mathcal{X}, \\ \aleph_2(t,\mathcal{X},\mathcal{Y},\mathcal{Z}) = p\Lambda - \frac{(1-\psi)\beta_2\mathcal{Y}\mathcal{Z}}{\mathcal{X}+\mathcal{Y}+\mathcal{Z}} - \mu_2\mathcal{Y}, \\ \aleph_3(t,\mathcal{X},\mathcal{Y},\mathcal{Z}) = \frac{\beta_1\mathcal{X}\mathcal{Z}}{\mathcal{X}+\mathcal{Y}+\mathcal{Z}} + \frac{(1-\psi)\beta_2\mathcal{Y}\mathcal{Z}}{\mathcal{X}+\mathcal{Y}+\mathcal{Z}} - \mu_3\mathcal{Z}, \end{cases} \tag{15}$$

which can be expressed as

$$\begin{cases} {}^{ABC}_{\ \ 0}D^{\xi}_{t}\aleph(t) = \eth(t,\aleph(t)), & t\in[0,T], \\ \aleph(0) = \aleph_0, & 0<\xi\leq 1, \end{cases} \tag{16}$$

where $\aleph(t) = (\mathcal{X}(t),\mathcal{Y}(t),\mathcal{Z}(t)^T$ and $\aleph_0 = (\mathcal{X}_0,\mathcal{Y}_0,\mathcal{Z}_0)^T$.

$${}^{ABC}_{\ \ 0}D^{\xi}_{t}\aleph(t) = \begin{cases} {}^{ABC}_{\ \ 0}D^{\xi}_{t}\mathcal{X}(t), \\ {}^{ABC}_{\ \ 0}D^{\xi}_{t}\mathcal{Y}(t), \\ {}^{ABC}_{\ \ 0}D^{\xi}_{t}\mathcal{Z}(t). \end{cases} \qquad \eth(t,\aleph(t)) = \begin{cases} \aleph_1(t,\mathcal{X},\mathcal{Y},\mathcal{Z}), \\ \aleph_2(t,\mathcal{X},\mathcal{Y},\mathcal{Z}), \\ \aleph_3(t,\mathcal{X},\mathcal{Y},\mathcal{Z}). \end{cases} \tag{17}$$

Let $\mathbb{P} = C([0,T],\mathbb{R})$ signify the Banach space consisting of all continuous functions from the interval $[0,T]$ to $\mathbb{R}$, endowed with the norm given as

$||\aleph|| = \max\limits_{t\in[0,T]}|\aleph(t)|$, where $|\aleph(t)| = |\mathcal{X}(t)| + \mathcal{Y}(t)| + |\mathcal{Z}(t)|$.

Based on Lemma 1, the solution of system (16) can be expressed as follows:

$$\aleph(t) = \aleph_0 + \frac{1-\xi}{ABC(\xi)}\eth(t,\aleph(t)) + \frac{\xi}{ABC(\xi)\Gamma(\xi)}\int_0^t (t-\tau)^{\xi-1}\eth(\tau,\aleph(\tau))d\tau. \tag{18}$$

Lemma 5. The following conditions are key to our analysis:

(I) There exist two positive constants $\mathfrak{W}_1,\ \mathfrak{W}_2$ such that

$$|\eth(t,\aleph(t))| \leq \mathfrak{W}_1||\aleph|| + \mathfrak{W}_2. \tag{19}$$

(II) There exists $\mathfrak{W}_3 > 0$ such that

$$|\eth(t, \aleph(t)) - \eth(t, \overline{\aleph}(t))| \leq \mathfrak{W}_3 |\aleph(t) - \overline{\aleph}(t)|. \tag{20}$$

Proof. From system (15), we have

$$\eth(t, \aleph(t)) = \begin{pmatrix} (1-p)\Lambda - \frac{\beta_1 \mathcal{X}\mathcal{Z}}{\mathcal{X}+\mathcal{Y}+\mathcal{Z}} - \mu_1 \mathcal{X} \\ p\Lambda - \frac{(1-\psi)\beta_2 \mathcal{Y}\mathcal{Z}}{\mathcal{X}+\mathcal{Y}+\mathcal{Z}} - \mu_2 \mathcal{Y} \\ \frac{\beta_1 \mathcal{X}\mathcal{Z}}{\mathcal{X}+\mathcal{Y}+\mathcal{Z}} + \frac{(1-\psi)\beta_2 \mathcal{Y}\mathcal{Z}}{\mathcal{X}+\mathcal{Y}+\mathcal{Z}} - \mu_3 \mathcal{Z} \end{pmatrix}. \tag{21}$$

Using the triangle inequality, we obtain

$$\begin{aligned} \left|\eth(t, \aleph(t))\right| \leq & \left|(1-p)\Lambda - \frac{\beta_1 \mathcal{X}\mathcal{Z}}{\mathcal{X}+\mathcal{Y}+\mathcal{Z}} - \mu_1 \mathcal{X}\right| \\ & + \left|p\Lambda - \frac{(1-\psi)\beta_2 \mathcal{Y}\mathcal{Z}}{\mathcal{X}+\mathcal{Y}+\mathcal{Z}} - \mu_2 \mathcal{Y}\right| \\ & + \left|\frac{\beta_1 \mathcal{X}\mathcal{Z}}{\mathcal{X}+\mathcal{Y}+\mathcal{Z}} + \frac{(1-\psi)\beta_2 \mathcal{Y}\mathcal{Z}}{\mathcal{X}+\mathcal{Y}+\mathcal{Z}} - \mu_3 \mathcal{Z}\right|. \end{aligned}$$

Again applying the triangle inequality gives

$$\begin{aligned} \left|\eth(t, \aleph(t))\right| \leq & \left|(1-p)\Lambda\right| + \beta_1 \mathbb{M}_1 + \mu_1 \left|\mathcal{X}\right| \\ & + \left|p\Lambda\right| + (1-\psi)\beta_2 \mathbb{M}_2 + \mu_2 \left|\mathcal{Y}\right| \\ & + \beta_1 \mathbb{M}_1 + (1-\psi)\beta_2 \mathbb{M}_2 + \mu_3 \left|\mathcal{Z}\right|, \end{aligned}$$

where $\mathbb{M}_1 = \max_{t\in[0,T]} \left|\frac{\mathcal{X}\mathcal{Z}}{\mathcal{X}+\mathcal{Y}+\mathcal{Z}}\right|$ and $\mathbb{M}_2 = \max_{t\in[0,T]} \left|\frac{\mathcal{Y}\mathcal{Z}}{\mathcal{X}+\mathcal{Y}+\mathcal{Z}}\right|$. □

Therefore,

$$\left|\eth(t, \aleph(t))\right| \leq \underbrace{\Lambda + 2\beta_1 \mathbb{M}_1 + 2(1-\psi)\beta_2 \mathbb{M}_2}_{\mathfrak{M}_2} + \underbrace{(\mu_1 + \mu_2 + \mu_3)}_{\mathfrak{M}_1} ||\aleph||,$$

$$\left|\eth(t, \aleph(t))\right| \leq \mathfrak{M}_1 ||\aleph|| + \mathfrak{M}_2.$$

Next, we prove condition (II). Let $\mathfrak{G} = \left\{(t, \aleph) | 0 \leq t \leq T, \aleph \in \mathbb{R}^3_+\right\}$ and let $\mathscr{U} \subseteq \mathfrak{G}$ be convex and compact. Let $\aleph, \overline{\aleph} \in \mathfrak{G}$. Then by the mean value theorem, there exists $\theta \in (\aleph, \overline{\aleph})$ such that

$$\begin{aligned}\frac{\eth(\aleph(t))-\eth(\overline{\aleph}(t))}{\aleph(t)-\overline{\aleph}(t)} &= \eth'(\theta(t)),\\ \eth(\aleph(t))-\eth(\overline{\aleph}(t)) &= \eth'(\theta(t))(\aleph(t)-\overline{\aleph}(t)),\\ \left|\eth(\aleph(t))-\eth(\overline{\aleph}(t))\right| &= \left|\eth'(\theta(t))(\aleph(t)-\overline{\aleph}(t))\right|\\ &\leq \left|\left|\eth'(\theta)\right|\right|_\infty \left|\left|\aleph-\overline{\aleph}\right|\right|.\end{aligned}$$

Since $\eth \in C^1[0,T]$, over convex compact set $\mathscr{U}$, there exists a constant $\mathfrak{M}_3 > 0$ such that

$$\left|\left|\eth'(\theta)\right|\right|_\infty \leq \mathfrak{M}_3,$$

hence,

$$\begin{aligned}\left|\eth(\aleph(t))-\eth(\overline{\aleph}(t))\right| &\leq \mathfrak{M}_3\left|\left|\aleph-\overline{\aleph}\right|\right|_\infty,\\ \max_{t\in[0,T]}\left|\eth(\aleph)-\eth(\overline{\aleph})\right| &\leq \mathfrak{M}_3\left|\left|\aleph-\overline{\aleph}\right|\right|_\infty,\\ \left|\left|\eth(\aleph)-\eth(\overline{\aleph})\right|\right|_\infty &\leq \mathfrak{M}_3\left|\left|\aleph-\overline{\aleph}\right|\right|_\infty.\end{aligned}$$

Hence $\eth(\aleph)$ is Lipschitz.

We start with the following result.

Lemma 6. Let us consider a map $\widehat{\mathscr{Q}}$ on $\mathbb{P}$ such that

$$\widehat{\mathscr{Q}}(\aleph(t)) = \aleph_0 + \tfrac{1-\xi}{ABC(\xi)}\eth(t,\aleph(t)) + \tfrac{\xi}{ABC(\xi)\Gamma(\xi)}\int_0^t (t-\tau)^{\xi-1}\eth(\tau,\aleph(\tau))d\tau. \tag{22}$$

Then it is completely continuous.

Proof. Initially, we observe that if $\widehat{\mathscr{Q}} \in \mathbb{P}$, then $\widehat{\mathscr{Q}}(\aleph) \in \mathbb{P}$. For all $\aleph \in \mathscr{M}_z = \{\aleph \in \mathbb{P} \ni ||\aleph|| \leq z\}$, we have

$$\begin{aligned}|\widehat{\mathscr{Q}}(\aleph(t))| \leq& ||\aleph_0|| + \frac{1-\xi}{ABC(\xi)}\max_{t\in[0,T]}|\eth(t,\aleph(t))|\\ &+ \max_{t\in[0,T]}|\frac{\xi}{ABC(\xi)\Gamma(\xi)} \times \int_0^t (t-\tau)^{\xi-1}\eth(\tau,\aleph(\tau))d\tau|\\ \leq& ||\aleph_0|| + \frac{1-\xi}{ABC(\xi)}(\mathfrak{W}_1||\aleph|| + \mathfrak{W}_2) + \frac{T^\xi}{ABC(\xi)\Gamma(\xi)}(\mathfrak{W}_1||\aleph|| + \mathfrak{W}_2)\\ \leq& ||\aleph_0|| + \left(\frac{1-\xi}{ABC(\xi)} + \frac{T^\xi}{ABC(\xi)\Gamma(\xi)}\right)\mathfrak{W}_2\end{aligned}$$

$$+\left(\frac{1-\xi}{ABC(\xi)}+\frac{T^{\xi}}{ABC(\xi)\Gamma(\xi)}\right)\mathfrak{W}_1||\aleph||$$
$$\leq||\aleph_0||+\daleth(\mathfrak{W}_1||\aleph||+\mathfrak{W}_2)<\infty, \tag{23}$$

where $\daleth=\left(\frac{1-\xi}{ABC(\xi)}+\frac{T^{\xi}}{ABC(\xi)\Gamma(\xi)}\right)$. This implies that $||\widehat{\mathscr{Q}}(\aleph)||<\infty$. Therefore, $\widehat{\mathscr{Q}}$ is uniformly bounded on $\mathscr{M}_z$.

Next, we establish that the operator $\widehat{\mathscr{Q}}$ is equicontinuous. To achieve this, let $\aleph\in\mathscr{M}_z$ and let $t_1,t_2\in[0,T]$ such that $t_1<t_2$. Then

$$\begin{aligned}|\widehat{\mathscr{Q}}\aleph(t_1)-\widehat{\mathscr{Q}}\aleph(t_2)|\leq&\max_{t\in[0,T]}\left|\frac{1-\xi}{ABC(\xi)}(\eth(t_1,\aleph(t_1))-\eth(t_2,\aleph(t_2))\right|\\&+\max_{t\in[0,T]}\frac{\xi}{ABC(\xi)\Gamma(\xi)}\left|\int_0^{t_1}(t_1-\tau)^{\xi-1}\eth(\tau,\aleph(\tau))d\tau\right.\\&\left.-\int_0^{t_2}(t_2-\tau)^{\xi-1}\eth(\tau,\aleph(\tau))d\tau\right|\\\leq&\frac{1-\xi}{ABC(\xi)}\max_{t\in[0,T]}\left|\eth(t_1,\aleph(t_1))-\eth(t_2,\aleph(t_2)\right|\\&+\frac{\mathfrak{W}_1||\aleph||+\mathfrak{W}_2}{ABC(\xi)\Gamma(\xi)}(t_2^{\xi}-t_1^{\xi}).\end{aligned} \tag{24}$$

It is evident that the right-hand side of the above inequality approaches zero as $t_1\to t_2$. The operator $\widehat{\mathscr{Q}}$ is equicontinuous, and from (23), the operator $\widehat{\mathscr{Q}}$ is uniformly bounded. Therefore, by the Arzela-Ascoli theorem, it follows that $\widehat{\mathscr{Q}}$ is relatively compact, implying that $\widehat{\mathscr{Q}}$ is completely continuous. □

Theorem 3. Model (11) has at least one solution.

Proof. Consider $\widehat{\Omega}$ such that

$$\widehat{\Omega}=\left\{\aleph\in\mathbb{P}\ni\aleph=\upsilon\widehat{\mathscr{Q}}(\aleph),\upsilon\in(0,1)\right\}.$$

In order to establish that the set $\widehat{\Omega}$ is bounded, suppose that $\aleph\in\mathscr{M}_z$, and confirm that the following inequality is satisfied for all $t\in[0,T]$:

$$||\aleph||=\upsilon||\widehat{\mathscr{Q}}(\aleph)||\leq\upsilon\left(|\aleph_0|+\left(\frac{1-\xi}{ABC(\xi)}+\frac{T^{\xi}}{ABC(\xi)\Gamma(\xi)}\right)\left[\mathfrak{W}_1||\aleph||+\mathfrak{W}_2\right]\right). \tag{25}$$

Hence, the set $\widehat{\Omega}$ is proven to be bounded. Therefore, by invoking Schaefer's fixed point theorem, we deduce that the operator $\widehat{\mathscr{Q}}(\aleph)$ possesses at least one fixed point. Consequently, the proposed pneumonia transmission model (11) admits at least one solution.

□

Theorem 4. The solution to (11) is guaranteed to be unique provided the following condition is satisfied:

$$\tfrac{1-\xi}{ABC(\xi)}\mathfrak{W}_3 + \tfrac{T^{\xi}}{ABC(\xi)\Gamma(\xi)}\mathfrak{W}_3 < 1. \tag{26}$$

Proof. To obtain the required result, we apply the Banach contraction theorem. Let $\aleph$, $\overline{\aleph} \in \mathbb{P}$, and assume that condition (II) holds. Then,

$$\begin{aligned}
||\widehat{\mathscr{Q}}\aleph - \widehat{\mathscr{Q}}\overline{\aleph}|| \leq & \max_{t\in[0,T]} |\frac{1-\xi}{ABC(\xi)}\eth(t,\aleph(t)) - \frac{1-\xi}{ABC(\xi)}\eth(t,\overline{\aleph}(t)) \\
& + \frac{\xi}{ABC(\xi)\Gamma(\xi)}\int_0^t (t-\tau)^{\xi-1}\eth(\tau,\aleph(\tau))d\tau \\
& + \frac{\xi}{ABC(\xi)\Gamma(\xi)}\int_0^t (t-\tau)^{\xi-1}\eth(\tau,\overline{\aleph}(\tau))d\tau| \\
\leq & \left(\frac{1-\xi}{ABC(\xi)}\mathfrak{W}_3 + \frac{T^{\xi}}{ABC(\xi)\mathfrak{W}_3}\right)||\aleph - \overline{\aleph}||.
\end{aligned} \tag{27}$$

As a result, we derive

$$||\widehat{\mathscr{Q}}\aleph - \widehat{\mathscr{Q}}\overline{\aleph}|| \leq \mathscr{B}||\aleph - \overline{\aleph}||, \tag{28}$$

where

$$\mathscr{B} = \tfrac{1-\xi}{ABC(\xi)}\mathfrak{W}_3 + \tfrac{T^{\xi}}{ABC(\xi)\Gamma(\xi)}\mathfrak{W}_3.$$

Therefore, we conclude that there exists a unique fixed point of $\widehat{\mathscr{Q}}$, which implies that system (11) admits a unique solution. □

5 UH stability

UH stability is crucial in ensuring that the solutions of fractional differential equations (FDEs) are resistant to small perturbations, which is essential when modeling systems with memory effects and nonlocal dynamics. This stability investigation helps determine whether small changes in the initial data or parameters lead to limited variations in the solutions, which is essential for verifying the reliability and strength of the proposed model. Recent research has applied UH stability to fractional functional differential equations and neutral fractional evolution equations with delay, demonstrating its significance in preserving the reliability and practical utility of fractional models in diverse fields, including biology and engineering.

We examine the stability of the proposed system by introducing a small perturbation $\mathfrak{F} \in C[0,T]$, which helps assess the system's response to minor changes. This analysis is essential for confirming the system's resilience under different conditions:

(a) $||\mathfrak{F}(t)|| \leq \varepsilon,\ \mathfrak{F} = \max(\mathfrak{F}_j)^T,\ t \in [0,T],\ j = 1,2,\ldots,5,$

(b) ${}^{ABC}_{\ \ 0}D^{\xi}_{t}\aleph(t) = \eth(t,\aleph(t)) + \mathfrak{F}(t),\ t \in [0,T].$

Lemma 7. The solution of the modified problem can be expressed as follows:

$$ {}^{ABC}_{\ \ 0}D^{\xi}_{t}\aleph(t) = \eth(t,\aleph(t)) + \mathfrak{F}(t), \qquad t \in [0,T], \tag{29} $$

with the initial condition

$\aleph(0) = \aleph_0,$

with the relationship

$$ \begin{aligned} &\Bigg|\Bigg|\aleph(t) - \Bigg(\aleph_0(t) + \tfrac{1-\xi}{ABC(\xi)}\eth(t,\aleph(t)) \\ &+ \frac{\xi}{ABC(\xi)\Gamma(\xi)}\int_0^t (t-\tau)^{\xi-1}\eth(\tau,\aleph(\tau))d\tau\Bigg)\Bigg|\Bigg| \leq \epsilon\mathfrak{U}, \end{aligned} \tag{30} $$

where $\mathfrak{U} = \frac{(\Gamma(\xi)(1-\xi)+T^{\xi})}{ABC(\xi)\Gamma(\xi)}$ holds true.

Proof. From (30), we have ${}^{ABC}_{\ \ 0}D^{\xi}_{t}\aleph(t) = \eth(t,\aleph(t)) + \mathfrak{F}(t),\ t \in [0,T]$. Now, we use Definition 5 and obtain

$$ \left.\begin{aligned} \aleph(t) = \aleph_0(t) + \tfrac{1-\xi}{ABC(\xi)}\eth(t,\aleph(t)) + \tfrac{\xi}{ABC(\xi)\Gamma(\xi)}\int_0^t (t-\tau)^{\xi-1}\eth(\tau,\aleph(\tau))d\tau \\ \tfrac{1-\xi}{ABC(\xi)}\mathfrak{F}(t) + \tfrac{\xi}{ABC(\xi)\Gamma(\xi)}\int_0^t (t-\tau)^{\xi-1}\mathfrak{F}(\tau)d\tau, \end{aligned}\right\} \tag{31} $$

$$\left.\begin{aligned}&\left|\left|\aleph(t)-\left(\aleph_0(t)+\tfrac{1-\xi}{ABC(\xi)}\eth(t,\aleph(t))+\tfrac{\xi}{ABC(\xi)\Gamma(\xi)}\int_0^t(t-\tau)^{\xi-1}\eth(\tau,\aleph(\tau))d\tau\right)\right|\right|\\&=\left|\left|\tfrac{1-\xi}{ABC(\xi)}\mathfrak{F}(t)+\tfrac{\xi}{ABC(\xi)\Gamma(\xi)}\int_0^t(t-\tau)^{\xi-1}\mathfrak{F}(\tau)d\tau\right|\right|.\end{aligned}\right\}\tag{32}$$

After simplification, we have

$$\left.\begin{aligned}&\left|\left|\aleph(t)-\left(\aleph_0(t)+\tfrac{1-\xi}{ABC(\xi)}\eth(t,\aleph(t))+\tfrac{\xi}{ABC(\xi)\Gamma(\xi)}\int_0^t(t-\tau)^{\xi-1}\eth(\tau,\aleph(\tau))d\tau\right)\right|\right|\\&\qquad\leq\epsilon\mathfrak{U},\end{aligned}\right\}$$

where $\mathfrak{U}=\frac{(\Gamma(\xi)(1-\xi)+T^{\xi})}{ABC(\xi)\Gamma(\xi)}$. □

Theorem 5. Assuming condition (II) and utilizing (30), the solution of the system (11) is demonstrated to exhibit UH stability. As a result, the analytical solution of the proposed system is confirmed to be UH stable when $\mathfrak{T}<1$, where $\mathfrak{T}=\mathfrak{W}_3\mathfrak{U}$.

Proof. Assuming that condition (II) is satisfied and that a unique solution exists, denoted as $\overline{\aleph}\in\mathbb{P}$ and considering any other solution $\aleph\in\mathbb{P}$ to (16), it follows that

$$\begin{aligned}&\left|\left|\aleph(t)-\overline{\aleph}(t)\right|\right|\\&=\left|\left|\aleph(t)-\left(\aleph_0(t)+\frac{1-\xi}{ABC(\xi)}\eth(t,\overline{\aleph}(t))\right.\right.\\&\qquad\left.\left.+\frac{\xi}{ABC(\xi)\Gamma(\xi)}\int_0^t(t-\tau)^{\xi-1}\eth(\tau,\overline{\aleph}(\tau))d\tau\right)\right|\right|.\end{aligned}\tag{33}$$

$$\left.\begin{aligned}&\left|\left|\aleph(t)-\overline{\aleph}(t)\right|\right|\\&\leq\left|\left|\aleph(t)-\left(\aleph_0(t)+\tfrac{1-\xi}{ABC(\xi)}\eth(t,\aleph(t))\right.\right.\\&\quad\left.\left.+\tfrac{\xi}{ABC(\xi)\Gamma(\xi)}\int_0^t(t-\tau)^{\xi-1}\eth(\tau,\aleph(\tau))d\tau\right)\right|\right|\\&\quad+\left|\left|\left(\aleph_0(t)+\tfrac{1-\xi}{ABC(\xi)}\eth(t,\aleph(t))+\tfrac{\xi}{ABC(\xi)\Gamma(\xi)}\int_0^t(t-\tau)^{\xi-1}\eth(\tau,\aleph(\tau))d\tau\right)\right.\right.\\&\quad\left.\left.-\left(\aleph_0(t)+\tfrac{1-\xi}{ABC(\xi)}\eth(t,\overline{\aleph}(t))+\tfrac{\xi}{ABC(\xi)\Gamma(\xi)}\int_0^t(t-\tau)^{\xi-1}\eth(\tau,\overline{\aleph}(\tau))d\tau\right)\right|\right|.\end{aligned}\right\}\tag{34}$$

$$\left|\left|\aleph(t)-\overline{\aleph}(t)\right|\right|\leq\frac{\mathfrak{U}\epsilon}{1-\mathfrak{T}},\tag{35}$$

where $\mathfrak{T} = \mathfrak{W}_3\mathfrak{U}$.

From (34), it follows that the solution of (11) is stable in the UH sense and, more generally, in the generalized UH sense, when $\mathfrak{Q}(\epsilon) = \mathfrak{U}\epsilon$ and $\mathfrak{Q}(0) = 0$. □

6 Disease-free equilibrium point and the basic reproduction number

The calculation of the equilibrium points (EPs) for the model described in (11) is outlined below. The equilibrium states represent points where the population sizes remain constant. First, we determine the EPs, followed by an analysis of the model's stability. The equilibrium states are obtained by solving the following equations:

$$\begin{cases} {}^{ABC}_{\ \ 0}D^{\xi}_{t}\mathcal{X}(t) = 0, \\ {}^{ABC}_{\ \ 0}D^{\xi}_{t}\mathcal{Y}(t) = 0, \\ {}^{ABC}_{\ \ 0}D^{\xi}_{t}\mathcal{Z}(t) = 0. \end{cases} \tag{36}$$

The disease-free equilibrium (DFE), denoted $\mathscr{P}^0 = \left(\mathcal{X}^0, \mathcal{Y}^0, \mathcal{Z}^0\right)$, refers to the state in which the illness is not present in the system. The DFE is given by the following expression:

$$\begin{cases} \mathcal{X}^0 & = \frac{\Lambda(1-p)}{\mu_1}, \\ \mathcal{Y}^0 & = \frac{\Lambda p}{\mu_2}, \\ \mathcal{Z}^0 & = 0. \end{cases} \tag{37}$$

The basic reproduction number, commonly referred to as $\mathfrak{R}_0$, is a key epidemiological parameter that indicates the average number of secondary infections caused by a single infected individual in a fully susceptible population. It is essential for understanding the potential for Pneumocystis Pneumonia to spread. To calculate $\mathfrak{R}_0$, the next-generation matrix method is used. As a result, $\mathfrak{R}_0$ can be expressed in the following form:

$$\mathfrak{R}_0 = \rho(\mathscr{F}\mathscr{V}^{-1}). \tag{38}$$

In this context, ρ represents the spectral radius of the matrix $\mathscr{F}\mathscr{V}^{-1}$, where $\mathscr{F}$ is the matrix of new infection terms and $\mathscr{V}$ is the matrix of transfer terms out of the infected compartment:

$$\mathscr{F} = \left(\frac{\beta_1 \mathcal{X}^0 + \beta_2(1-\psi)\mathcal{Y}^0}{\mathcal{X}^0 + \mathcal{Y}^0}\right), \qquad \mathscr{V} = \mu_3. \tag{39}$$

Therefore, $\mathfrak{R}_0$ can be represented as $\mathfrak{R}_0 = \rho(\mathscr{F}\mathscr{V}^{-1}) = \left(\frac{\beta_1 \mathcal{X}^0 + \beta_2(1-\psi)\mathcal{Y}^0}{\mu_3(\mathcal{X}^0+\mathcal{Y}^0)}\right) = \frac{\beta_2\mu_1 p(1-\psi)+\beta_1\mu_2(1-p)}{\mu_3(\mu_1 p+\mu_2(1-p))}$.

The analytical expression obtained for the basic reproduction number $\mathfrak{R}_0$ reveals that it is governed by several key parameters of the model. A value of $\mathfrak{R}_0 > 1$ indicates that there is a transmission of the disease between the immune-deficient population that can be sustained. This is because on average an infectious individual gives rise to more than one secondary case. However, the situation is reversed when $\mathfrak{R}_0 < 1$ and the disease will slowly disappear in the population. The magnitude of $\mathfrak{R}_0$ is affected by multiple factors, including the average duration of infectiousness (associated with $\frac{1}{\mu_3}$), the transmission coefficients β_1 and β_2, as well as control-related parameters such as prophylaxis uptake p and its effectiveness ψ. Owing to its central role in epidemiological analysis, $\mathfrak{R}_0$ serves as a fundamental indicator for evaluating intervention strategies and informing public health decision-making, particularly for protecting high-risk populations vulnerable to Pneumocystis pneumonia.

We investigate the effect of two-parameter variations on the value of the basic reproduction number. Figures 2(a) and 2(b) show that prophylaxis efficacy and prophylaxis coverage lead to $\mathfrak{R}_0 < 1$, indicating the disease-free state in the region

6.1 Existence of endemic equilibrium point

The endemic equilibrium $\mathscr{P}^* = \left(\mathcal{X}^*, \mathcal{Y}^*, \mathcal{Z}^*\right)$ corresponds to a steady state in which Pneumocystis Pneumonia remains present within the population, characterized by a strictly positive level of infection. This scenario is of high concern, as it reflects sustained transmission. At steady state, we can consider $\mathscr{N}^* = \mathcal{X}^* + \mathcal{Y}^* + \mathcal{Z}^* = \mathcal{X}^0 + \mathcal{Y}^0 + \mathcal{Z}^0 = \frac{\Lambda(1-p)\mu_2+\Lambda p}{\mu_1\mu_2}$ which is a constant total population. The components of the EEP can be expressed as follows:

$$\begin{cases} \mathcal{X}^* = \frac{\Lambda(1-p)\mathscr{N}^*}{\beta_1\mathcal{Z}^*+\mu_1\mathscr{N}^*}, \\ \mathcal{Y}^* = \frac{\Lambda p\mathscr{N}^*}{\beta_2(1-\psi)\mathcal{Z}^*+\mu_2\mathscr{N}^*}. \end{cases} \tag{40}$$

To determine the positive solution $\mathcal{Z}^*$, the expressions for $\mathcal{X}^*$ and $\mathcal{Y}^*$ given in (40), together with $\mathcal{Z}^* = \mathscr{N}^* - \mathcal{X}^* + \mathcal{Y}^*$, are substituted into the third equation of system (11). This substitution leads to a quadratic equation in $\mathcal{Z}^*$,

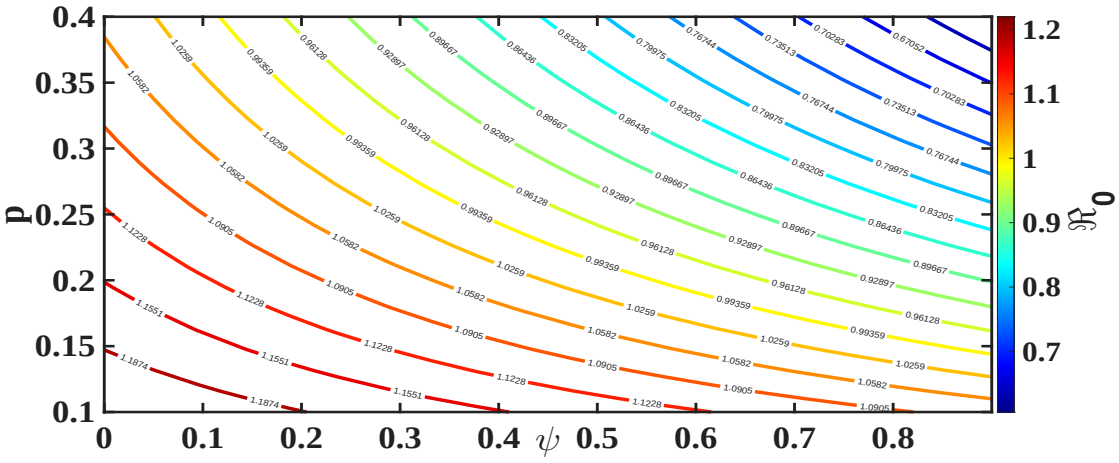

(a)

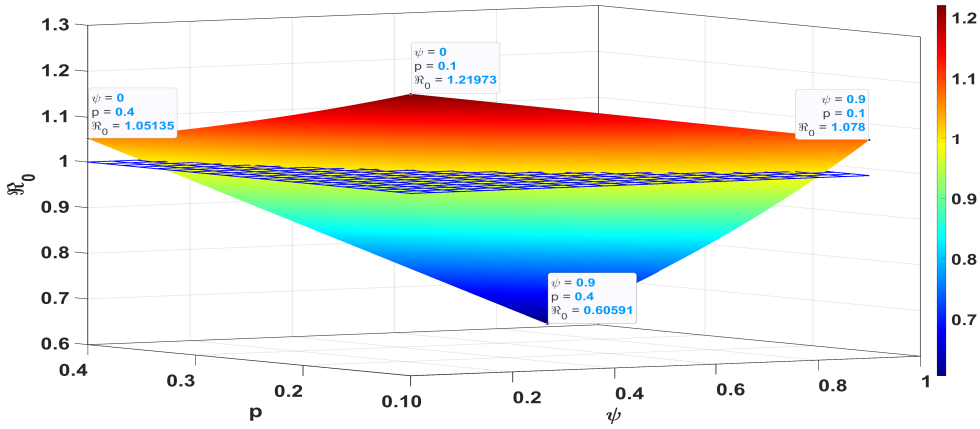

(b)

Figure 2: The impact of parameters ψ and p on $\mathfrak{R}_0$

$$\mathcal{Q}(\mathcal{Z}^*) = \mathscr{A}(\mathcal{Z}^*)^2 + \mathscr{B}(\mathcal{Z}^*) + \mathscr{C}, \tag{41}$$

where

$$\begin{cases} \mathscr{A} = \beta_1\beta_2\mu_3(1-\psi), \\ \mathscr{B} = \beta_2(1-\psi)(\mu_3\mu_1\mathcal{N}^* - \beta_1\Lambda) + \beta_1\mu_2\mu_3\mathcal{N}^*, \\ \mathscr{C} = \mu_1\mu_2\mu_3(\mathcal{N}^*)^2 + \mu_1\Lambda\beta_2 p\mathcal{N}^*(\psi-1) + \beta_1\mu_2\Lambda(p-1)\mathcal{N}^* \\ \quad = \mu_1\mu_2\mu_3\mathcal{N}^*(\mathcal{X}^0+\mathcal{Y}^0)\left(\frac{\mathcal{N}^*}{(\mathcal{X}^0+\mathcal{Y}^0)} - \mathfrak{R}_0\right). \end{cases} \tag{42}$$

An endemic equilibrium exists if there is at least one positive real root for $\mathcal{Z}^*$. The existence of such a root depends on the signs of the coefficients $\mathscr{A}$, $\mathscr{B}$, and $\mathscr{C}$, it is easily seen that $\mathscr{A}$ always positive and $\mathscr{C}$ is negative whenever $\mathfrak{R}_0 > 1$. By the Descartes rule of signs, the polynomial (41) has a positive root, and an endemic equilibrium becomes feasible when $\mathfrak{R}_0 > 1$.

6.2 Local stability of equilibria

In the following part, we devote our attention to examining the stability of the EPs. Stability analysis determines whether the population will return to an equilibrium state after a small disturbance, such as the introduction of a few infected individuals. To begin, we present the theorem below which is fundamental for fractional-order systems.

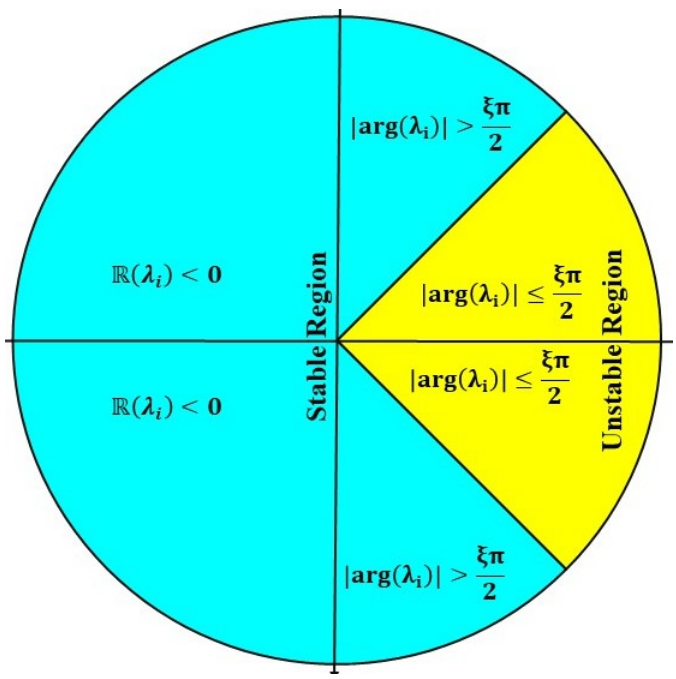

Figure 3: Stable region for fractional-order model.

Figure 3 displays the regions of stability (indicated in blue) and instability (indicated in yellow) for a fractional-order system defined by the order ξ. Figure 3 shows that the stability region for the fractional-order system is considerably larger than that of an integer-order system. Specifically, the integer-order system is stable only if all eigenvalues have negative real parts, which covers parts of the second and third quadrants. In contrast, the fractional-order system

exhibits a more extensive stability domain that extends beyond this axis. Therefore, while the stability of the integer-order model guarantees stability for the corresponding fractional-order model, the reverse is not true; a stable fractional-order model does not ensure the stability of the integer-order version.

Theorem 6. We begin by examining the following system of fractional order:

$$ {}^{ABC}_{0}D^{\xi}_{t}\mathcal{F}(t) = \mathscr{M}(t, \mathcal{F}(t)). \tag{43} $$

Suppose that $\mathcal{F}^*$ is an EP of the system given in (43), with $\mathcal{J}(\mathcal{F}^*)$ representing the Jacobian matrix evaluated at $\mathcal{F}^*$, $\lambda_i (i = 1, 2, \ldots, n)$ denoting its eigenvalues. Under these conditions, the system satisfies the following criteria:

(a) The EP $\mathcal{F}^*$ is locally asymptotically stable if each eigenvalue λ_i satisfies the condition $|arg(\lambda_i)| > \frac{\xi\pi}{2}$.

(b) The EP $\mathcal{F}^*$ is deemed unstable if there exists at least one eigenvalue λ_k, for some $k \in \{1, 2, \ldots, n\}$.

Next, we proceed to analyze the local stability of each EP individually. The Jacobian matrix corresponding to the DFE point is expressed in the following form:

$$ \mathcal{J}(\mathscr{P}^0) = \begin{pmatrix} -\mu_1 & 0 & -\frac{\beta_1(\beta_2(\psi-1)+\mu_3\mathfrak{R}_0)}{\beta_2(\psi-1)+\beta_1} \\ 0 & -\mu_2 & \frac{\beta_2(\psi-1)(\beta_1-\mu_3\mathfrak{R}_0)}{\beta_2(\psi-1)+\beta_1} \\ 0 & 0 & \mu_3(\mathfrak{R}_0 - 1) \end{pmatrix}. \tag{44} $$

The eigenvalues of $\mathcal{J}(\mathscr{P}^0)$ are $\lambda_1 = -\mu_1$, $\lambda_2 = -\mu_2$ and $\lambda_3 = \mu_3(\mathfrak{R}_0 - 1)$. It is easily seen that eigenvalues are negative if and only if $\mathfrak{R}_0 < 1$, establishing that the DFE $\mathscr{P}^0$ is locally asymptotically stable.

The Jacobian matrix evaluated at the endemic EPs $\mathscr{P}^*$ is given by

$$ \mathcal{J}(\mathscr{P}^*) = \begin{pmatrix} -\frac{\beta_1\mathcal{Z}^*(\mathcal{Z}^*+\mathcal{Y}^*)}{(\mathcal{X}^*+\mathcal{Y}^*+\mathcal{Z}^*)^2} - \mu_1 & \frac{\beta_1\mathcal{X}^*\mathcal{Z}^*}{(\mathcal{X}^*+\mathcal{Y}^*+\mathcal{Z}^*)^2} & -\frac{\beta_1\mathcal{X}^*(\mathcal{X}^*+\mathcal{Y}^*)}{(\mathcal{X}^*+\mathcal{Y}^*+\mathcal{Z}^*)^2} \\ -\frac{\beta_2(\psi-1)\mathcal{Z}^*\mathcal{Y}^*}{(\mathcal{Z}^*+\mathcal{Z}^*+\mathcal{Z}^*)^2} & \frac{\beta_2(\psi-1)\mathcal{Z}^*(\mathcal{X}^*+\mathcal{Z}^*)}{(\mathcal{X}^*+\mathcal{Y}^*+\mathcal{Z}^*)^2} - \mu_2 & \frac{\beta_2(\psi-1)\mathcal{Y}^*(\mathcal{X}^*+\mathcal{Y}^*)}{(\mathcal{X}^*+\mathcal{Y}^*+\mathcal{Z}^*)^2} \\ \frac{\mathcal{Z}^*(\beta_1(\mathcal{Z}^*+\mathcal{Y}^*)+\beta_2(\psi-1)\mathcal{Y}^*)}{(\mathcal{X}^*+\mathcal{Y}^*+\mathcal{Z}^*)^2} & -\frac{\mathcal{Z}^*(\beta_2(\psi-1)(\mathcal{X}^*+\mathcal{Z}^*)+\beta_1\mathcal{Z}^*)}{(\mathcal{X}^*+\mathcal{Y}^*+\mathcal{Z}^*)^2} & \frac{-\mu_3(\mathcal{X}^*+\mathcal{Y}^*+\mathcal{Z}^*)^2-\beta_2(\psi-1)\mathcal{Y}^*(\mathcal{X}^*+\mathcal{V}^*)+\beta_1}{(\mathcal{X}^*+\mathcal{Y}^*+\mathcal{Z}^*)^2} \end{pmatrix}, \tag{45} $$

$$\mathcal{J}(\mathscr{P}^*) = \begin{pmatrix} j_{11} & j_{12} & j_{13} \\ j_{21} & j_{22} & j_{23} \\ j_{31} & j_{32} & j_{33} \end{pmatrix}.$$

The characteristic equation of $\mathcal{J}(\mathscr{P}^*)$ is given by

$$\lambda^3 + p_1\lambda^2 + p_2\lambda + p_3 = 0, \tag{46}$$

where

$$\begin{aligned} p_1 &= j_{11} + j_{22} + j_{33}, \\ p_2 &= j_{22}j_{33} - j_{32}j_{23} + j_{11}j_{33} - j_{31}j_{13} + j_{11}j_{22} - j_{22}j_{12}, \\ p_3 &= j_{11}(j_{22}j_{33} - j_{32}j_{23}) - j_{12}(j_{22}j_{33} - j_{31}j_{23}) + j_{13}(j_{22}j_{32} - j_{31}j_{22}). \end{aligned}$$

If $p_1 > 0, p_2 > 0$, and $p_3 > 0$ with $p_1p_2 - p_3 > 0$, then all eigenvalues of $\mathcal{J}(\mathscr{P}^*)$ would lie in the left half-plane; hence the endemic equilibrium is locally asymptotically stable.

7 Sensitivity index

This section explores how variations in these parameters affect the transmission dynamics of the disease through sensitivity analysis. This process identifies which parameters have the most significant impact on $\mathfrak{R}_0$, thereby highlighting the most effective targets for control interventions. The parameter space is defined as

$$\mathbb{W} = \{(p, \beta_1, \beta_2, \psi, \mu_1, \mu_2, \mu_3) \in \mathbb{R}_+^7\}, \tag{47}$$

where $\mathfrak{R}_0 \in C^1(\mathbb{W})$. To evaluate how variations in a parameter $\eta \in \mathbb{W}$ influence $\mathfrak{R}_0$, we introduce the normalized forward sensitivity index, defined as

$$\mathcal{A}_\eta^{\mathfrak{R}_0} = \frac{\partial \mathfrak{R}_0}{\partial \eta} \times \frac{\eta}{\mathfrak{R}_0}. \tag{48}$$

This index quantifies the percentage change in $\mathfrak{R}_0$ resulting from a 1% change in the parameter η. A positive index means $\mathfrak{R}_0$ increases as the parameter increases, while a negative index

means that $\mathfrak{R}_0$ decreases. This analysis is crucial for prioritizing public health strategies for Pneumocystis Pneumonia control. This leads us to the following results:

$$
\begin{aligned}
\mathcal{A}_p^{\mathfrak{R}_0} &= \frac{\partial \mathfrak{R}_0}{\partial p} \times \frac{p}{\mathfrak{R}_0} \\
&= \frac{p\mu_3(p\mu_1 + \mu_2(1-p))\left(\frac{\mu_1\beta_2(1-psi)-\beta_1\mu_2}{\mu_3(\mu_1 p+\mu_2(1-p))} - \frac{(\beta_2\mu_1 p(1-psi)+\beta_1\mu_2(1-p))(\mu_1-\mu_2)}{\mu_3(\mu_1 p+\mu_2(1-p))^2}\right)}{p\mu_1\beta_2(1-\psi)+\beta_1\mu_2(1-p)}, \\
\mathcal{A}_{\beta_1}^{\mathfrak{R}_0} &= \frac{\partial \mathfrak{R}_0}{\partial \beta_1} \times \frac{\beta_1}{\mathfrak{R}_0} \\
&= \frac{\beta_1\mu_2(1-p)}{\beta_2\mu_1 p(1-\psi)+\beta_1\mu_2(1-p)}, \\
\mathcal{A}_{\beta_2}^{\mathfrak{R}_0} &= \frac{\partial \mathfrak{R}_0}{\partial \beta_2} \times \frac{\beta_2}{\mathfrak{R}_0} \\
&= \frac{\beta_2\mu_1 p(1-\psi)}{\beta_2\mu_1 p(1-\psi)+\beta_1\mu_2(1-p)}, \\
\mathcal{A}_{\psi}^{\mathfrak{R}_0} &= \frac{\partial \mathfrak{R}_0}{\partial \psi} \times \frac{\psi}{\mathfrak{R}_0} \\
&= -\frac{\beta_2\mu_1 p\psi}{\beta_2\mu_1 p(1-\psi)+\beta_1\mu_2(1-p)}, \\
\mathcal{A}_{\mu_1}^{\mathfrak{R}_0} &= \frac{\partial \mathfrak{R}_0}{\partial \mu_1} \times \frac{\mu_1}{\mathfrak{R}_0} \\
&= \frac{\mu_1\mu_3(\mu_1 p + \mu_2(1-p))\left(\frac{p\beta_2(1-\psi)}{\mu_3(\mu_1 p+\mu_2(1-p))} - \frac{p(\beta_2\mu_1 p(1-\psi)+\beta_1\mu_2(1-p))}{\mu_3(\mu_1 p+\mu_2(1-p))^2}\right)}{\beta_2\mu_1 p(1-\psi)+\beta_1\mu_2(1-p)}, \\
\mathcal{A}_{\mu_2}^{\mathfrak{R}_0} &= \frac{\partial \mathfrak{R}_0}{\partial \mu_2} \times \frac{\mu_2}{\mathfrak{R}_0} \\
&= \frac{\mu_2\mu_3(\mu_1 p + \mu_2(1-p))\left(\frac{\beta_1(1-p)}{\mu_3(\mu_1 p+\mu_2(1-p))} - \frac{p(\beta_2\mu_1 p(1-\psi)+\beta_1\mu_2(1-p))}{\mu_3(\mu_1 p+\mu_2(1-p))^2}\right)}{\beta_2\mu_1 p(1-\psi)+\beta_1\mu_2(1-p)}, \\
\mathcal{A}_{\mu_3}^{\mathfrak{R}_0} &= \frac{\partial \mathfrak{R}_0}{\partial \mu_3} \times \frac{\mu_3}{\mathfrak{R}_0} = -1.
\end{aligned}
$$

The sensitivity of the basic reproduction number with respect to the model parameters is illustrated in Figure 4, where the normalized sensitivity indices identify the parameters that have the greatest influence on disease transmission.

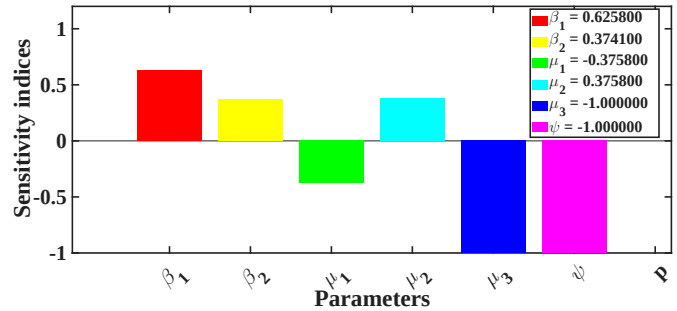

Figure 4: Sensitivity indices of $\mathfrak{R}_0$

8 Numerical scheme

The numerical simulations of the proposed fractional-order pneumonia model are performed using the numerical method developed by Solís-Pérez et al. [40]. This method is based on two-step Lagrange polynomial interpolation and is applied to the ABC fractional system (11) to investigate its dynamical behavior. An error and convergence analysis is also carried out to establish the convergence behavior of the implemented numerical scheme. This approach is as follows:

$$ {}^{ABC}_{\ \ 0}D^{\xi}_{t}\aleph(t) = \eth(t, \aleph(t)). \tag{49} $$

An equivalent integral representation of the fractional-order differential equation (49) is derived via the fundamental theorem of fractional calculus.

$$ \aleph(t) - \aleph(0) = \frac{1-\xi}{ABC(\xi)}\eth(t, \aleph(t)) + \frac{\xi}{ABC(\xi)\Gamma(\xi)}\int_0^t (t-\tau)^{\xi-1}\eth(\tau, \aleph(\tau))d\tau, \tag{50} $$

where $ABC(\xi) = 1 - \xi + \frac{\xi}{\Gamma(\xi)}$ is the normalization function. Equation (50) can be rewritten as

$$ \begin{aligned} \aleph(t_{j+1}) - \aleph(0) =& \frac{\Gamma(\xi)(1-\xi)}{\Gamma(\xi)(1-\xi)+\xi}\eth(t_j, \aleph(t_j)) \\ &+ \frac{\xi}{\Gamma(\xi)+\xi(1-\Gamma(\xi))}\sum_{n=0}^{j}\int_{t_n}^{t_{n+1}} \eth(\tau, \aleph(\tau)(t_{n+1}-\tau)^{\tau-1}d\tau. \end{aligned} \tag{51} $$

The function $\eth(\tau, \aleph(\tau))$ has an approximate value obtained by the two-step Lagrange polynomial interpolation. Throughout the range $[t_n, t_{n+1}]$.

$$\mathfrak{G}_m(\tau) \simeq \frac{\eth(t_n, \aleph_n)}{h}(\tau - t_{n-1}) - \frac{\eth(t_{n-1}, \aleph_{n-1})}{h}(\tau - t_n). \tag{52}$$

Now, taking into account (52) and (51), we arrive at

$$\left.\begin{aligned} \aleph_{j+1}(t) = \quad & \aleph_0 + \tfrac{(1-\xi)\Gamma(\xi)}{\xi+(1-\xi)\Gamma(\xi)}\eth(t_j, \aleph(t_j)) + \tfrac{\xi}{\Gamma(\xi)+\xi(1-\Gamma(\xi))} \\ & + \sum_{n=0}^{j}\Bigg(\frac{\eth(t_n, \aleph_n)}{h}\int_{t_n}^{t_{n+1}}(\tau - t_{n-1})(t_{j+1} - \tau)^{\xi-1}d\tau \\ & - \tfrac{\eth(t_{n-1}, \aleph_{n-1})}{h}\int_{t_n}^{t_{n+1}}(\tau - t_n)(t_{j+1} - \tau)^{\xi-1}d\tau\Bigg). \end{aligned}\right\} \tag{53}$$

For simplicity, we let

$$\left.\begin{aligned} \mathfrak{B}_{\xi,n,1} &= \int_{t_n}^{t_{n+1}}(\tau - t_{n-1})(t_{j+1} - \tau)^{\xi-1}d\tau, \\ \mathfrak{B}_{\xi,n,2} &= \int_{t_n}^{t_{n+1}}(\tau - t_n)(t_{j+1} - \tau)^{\xi-1}d\tau, \end{aligned}\right\} \tag{54}$$

which implies that

$$\left.\begin{aligned} \mathfrak{B}_{\xi,n,1} &= h^{\xi+1}\tfrac{(j+1-n)^{\xi}(j-n+2+\xi)-(j-n)^{\xi}(j-n+2-2\xi)}{\xi(\xi+1)}, \\ \mathfrak{B}_{\xi,n,2} &= h^{\xi+1}\tfrac{(j+1-n)^{j+1}-(j-n)^{\xi}(j-n+1+\xi)}{\xi(\xi+1)}. \end{aligned}\right\} \tag{55}$$

Substituting the integration (55) into (53), provides a viable approximation

$$\left.\begin{aligned} \aleph_{j+1}(t) = \quad & \aleph_0 + \tfrac{(1-\xi)\Gamma(\xi)}{\xi+(1-\xi)\Gamma(\xi)}\eth(t_j, \aleph(t_j)) + \tfrac{1}{\xi+(1+\xi)(1-\xi)\Gamma(\xi)} \\ & \times\sum_{n=0}^{j}\Bigg(h^{\xi}\eth(t_n, \aleph_n)\big((j+1-n)^{\xi}(j-n+2+\xi) \\ & -(j-n)^{\xi}(j-n+2+2\xi)\big) - h^{\xi}\eth(t_{n-1}, \aleph_{n-1})\big((j+1-n)^{\xi+1} \\ & -(j-n)^{\xi} \times (j-n+1+\xi)\big)\Bigg). \end{aligned}\right\} \tag{56}$$

Finally, the numerical solution of model (11) is found as follows:

$$\left.\begin{aligned}\mathcal{X}_{j+1}(t) = \;& \mathcal{X}_0 + \tfrac{(1-\xi)\Gamma(\xi)}{\xi+(1-\xi)\Gamma(\xi)}\aleph_1(t_j,\mathcal{X}(t_j),\mathcal{Y}(t_j),\mathcal{Z}(t_j)) + \tfrac{1}{\xi+(1+\xi)(1-\xi)\Gamma(\xi)}\\ & \times\sum_{n=0}^{j}\Bigg(h^{\xi}\aleph_1(t_n,\mathcal{X}_n,\mathcal{Y}_n,\mathcal{Z}_n)\big((j+1-n)^{\xi}(j-n+2+\xi)\\ & -(j-n)^{\xi}(j-n+2+2\xi)\big)\\ & -h^{\xi}\aleph_1(t_{n-1},\mathcal{X}_{n-1},\mathcal{Y}_{n-1},\mathcal{Z}_{n-1})\big((j+1-n)^{\xi+1}\\ & -(j-n)^{\xi}\times(j-n+1+\xi)\big)\Bigg),\end{aligned}\right\} \tag{57}$$

$$\left.\begin{aligned}\mathcal{Y}_{j+1}(t) = \;& \mathcal{Y}_0 + \tfrac{(1-\xi)\Gamma(\xi)}{\xi+(1-\xi)\Gamma(\xi)}\aleph_2(t_j,\mathcal{X}(t_j),\mathcal{Y}(t_j),\mathcal{Z}(t_j)) + \tfrac{1}{\xi+(1+\xi)(1-\xi)\Gamma(\xi)}\\ & \times\sum_{n=0}^{j}\Bigg(h^{\xi}\aleph_2(t_n,\mathcal{X}_n,\mathcal{Y}_n,\mathcal{Z}_n)\big((j+1-n)^{\xi}(j-n+2+\xi)\\ & -(j-n)^{\xi}(j-n+2+2\xi)\big)\\ & -h^{\xi}\aleph_2(t_{n-1},\mathcal{X}_{n-1},\mathcal{Y}_{n-1},\mathcal{Z}_{n-1})\big((j+1-n)^{\xi+1}\\ & -(j-n)^{\xi}\times(j-n+1+\xi)\big)\Bigg),\end{aligned}\right\} \tag{58}$$

$$\left.\begin{aligned}\mathcal{Z}_{j+1}(t) = \;& \mathcal{Z}_0 + \tfrac{(1-\xi)\Gamma(\xi)}{\xi+(1-\xi)\Gamma(\xi)}\aleph_3(t_j,\mathcal{X}(t_j),\mathcal{Y}(t_j),\mathcal{Z}(t_j)) + \tfrac{1}{\xi+(1+\xi)(1-\xi)\Gamma(\xi)}\\ & \times\sum_{n=0}^{j}\Bigg(h^{\xi}\aleph_3(t_n,\mathcal{X}_n,\mathcal{Y}_n,\mathcal{Z}_n)\big((j+1-n)^{\xi}(j-n+2+\xi)\\ & -(j-n)^{\xi}(j-n+2+2\xi)\big)\\ & -h^{\xi}\aleph_3(t_{n-1},\mathcal{X}_{n-1},\mathcal{Y}_{n-1},\mathcal{Z}_{n-1})\big((j+1-n)^{\xi+1}\\ & -(j-n)^{\xi}\times(j-n+1+\xi)\big)\Bigg).\end{aligned}\right\} \tag{59}$$

8.1 Error analysis

We now present the error analysis to validate the proposed scheme. Assuming that the function $\eth(t,\aleph(t))$ is twice differentiable, our given problem is as follows:

$$\begin{cases} {}^{ABC}_{\;\;0}D_t^{\xi}\aleph(t) = \eth(t,\aleph(t)), & t\in K=[0,T],\\ \aleph(0)=\aleph_0, & 0<\xi\leq 1.\end{cases}$$

The operator involved possesses a nonlocal and nonsingular kernel. Assuming that the function has a bounded second derivative, (16) can be reformulated as follows:

$$\begin{aligned}
\aleph(t_{k+1}) - \aleph(0) =& \frac{1-\xi}{ABC(\xi)}\eth(t_k, \aleph(t_k)) + \frac{\xi}{ABC(\xi)\Gamma(\xi)} \\
&\times \int_0^{t_{k+1}} \eth(\mathfrak{y}, \aleph(\mathfrak{y}))(t_{k+1}-\mathfrak{y})^{\xi-1} d\mathfrak{y} \\
=& \frac{1-\xi}{ABC(\xi)}\eth(t_k, \aleph(t_k)) + \frac{\xi}{ABC(\xi)\Gamma(\xi)} \\
&\times \sum_{n=0}^{k} \int_{t_n}^{t_{n+1}} \eth(\mathfrak{y}, \aleph(\mathfrak{y}))(t_{k+1}-\mathfrak{y})^{\xi-1} d\mathfrak{y} \\
=& \frac{1-\xi}{ABC(\xi)}\eth(t_k, \aleph(t_k)) + \frac{\xi}{ABC(\xi)\Gamma(\xi)} \\
&\times \sum_{n=0}^{k} \int_{t_n}^{t_{n+1}} \left\{ P_n(\mathfrak{y}) + \frac{(\mathfrak{y}-t_n)(\mathfrak{y}-t_{n-1})}{2!} \frac{\partial^2}{\partial \mathfrak{y}^2}[\eth(\mathfrak{y}, \aleph(\mathfrak{y}))]_{\mathfrak{y}=\gamma_n} \right\} \\
&\times (t_{k+1}-\mathfrak{y})^{\xi-1} d\mathfrak{y} \frac{1-\xi}{ABC(\xi)}\eth(t_k, \aleph(t_k)) + E_k^{\xi} + \frac{\xi}{ABC(\xi)\Gamma(\xi)} \\
&\sum_{n=0}^{k} \left\{ \frac{\eth(t_n, \aleph^n)}{h} \int_{t_n}^{t_{n+1}} (\mathfrak{y}-t_{n-1})(t_{k+1}-\mathfrak{y})^{\xi-1} d\mathfrak{y} \right. \\
&\left. - \frac{\eth(t_{n-1}, \aleph^{n-1})}{h} \int_{t_n}^{t_{n+1}} (\mathfrak{y}-t_n)(t_{k+1}-\mathfrak{y})^{\xi-1} d\mathfrak{y} \right\},
\end{aligned} \tag{60}$$

where

$$\begin{aligned}
E_k^{\xi} =& \frac{\xi}{ABC(\xi)\Gamma(\xi)} \sum_{n=0}^{k} \int_{t_n}^{t_{n+1}} \frac{(\mathfrak{y}-t_n)(\mathfrak{y}-t_{n-1})}{2!} \\
&\times \frac{\partial^2}{\partial \mathfrak{y}^2}[\eth(\mathfrak{y}, \aleph(\mathfrak{y}))]_{\mathfrak{y}=\gamma_n} (t_{k+1}-\mathfrak{y})^{\xi-1} d\mathfrak{y}.
\end{aligned} \tag{61}$$

One can find a point $\gamma_n \in [t_n, t_{n+1}]$ such that

$$\begin{aligned}
E_k^{\xi} =& \frac{\xi}{ABC(\xi)\Gamma(\xi)} \sum_{n=0}^{k} \frac{\partial^2}{\partial \mathfrak{y}^2}[\eth(\mathfrak{y}, \aleph(\mathfrak{y}))]_{\mathfrak{y}=\gamma_n} \frac{(\gamma_n - t_n)}{2} \\
&\times \int_{t_n}^{t_{n+1}} (\mathfrak{y}-t_{n-1})(t_{k+1}-\mathfrak{y})^{\xi-1} d\mathfrak{y} \\
=& \frac{\xi}{ABC(\xi)\Gamma(\xi)} \sum_{n=0}^{k} \frac{\partial^2}{\partial \mathfrak{y}^2}[\eth(\mathfrak{y}, \aleph(\mathfrak{y}))]_{\mathfrak{y}=\gamma_n} \frac{(\gamma_n - t_n)}{2} h^{\xi+1} \\
&\times \frac{1}{\xi(\xi+1)} \Big[(k-n+1)^{\xi}(k-n+2+\xi) - (k-n)^{\xi}(k-n+2+2\xi) \Big].
\end{aligned} \tag{62}$$

Taking the norm on both sides of (62), we obtain the following inequality:

$$||E_k^{\xi}|| \leq \frac{\xi h^{\xi+2}}{2ABC(\xi)\Gamma(\xi+2)} \underset{\mathfrak{y}\in[0,t_{k+1}]}{Sup} \left|\frac{\partial^2}{\partial \mathfrak{y}^2}\eth(\mathfrak{y},\aleph(\mathfrak{y}))\right| \times \sum_{n=0}^{k}\left|\left[(k-n+1)^{\xi}(k-n+2+\xi)-(k-n)^{\xi}(k-n+2+2\xi)\right]\right|. \tag{63}$$

Thus, we can calculate the error as follows:

$$||E_k^{\xi}|| \leq \frac{\xi h^{\xi+2}}{2ABC(\xi)\Gamma(\xi+2)} \underset{\mathfrak{y}\in[0,t_{k+1}]}{Sup} \left|\frac{\partial^2}{\partial \mathfrak{y}^2}\eth(\mathfrak{y},\aleph(\mathfrak{y}))\right| \times [(k+1)^{\xi}-\xi k^{\xi}]\frac{k(k+4+2\xi)}{2}. \tag{64}$$

From the derived error bound, it is evident that the numerical scheme exhibits a convergence rate of $\mathscr{O}(h^{\xi+2})$.

8.2 Computational experiments and results

Figures 5(a) and 5(b) show that increasing the fractional order leads to upward trends in the susceptible and prophylaxis-protected populations over time, respectively. However, Figure 5(c) reflects an opposite scenario in which a higher fractional order is associated with a decreasing trend in the infected population. This means that elevating the fractional order is beneficial for increasing the number of noninfected individuals. At the same time, it is a hindrance to the spread among the infected class. This behavior can be explained through the memory effect inherent in the Atangana–Baleanu fractional derivative. A smaller value of ξ corresponds to a stronger memory effect, implying that the influence of past infection states persists for a longer duration. Consequently, the force of infection from previously infected individuals continues to affect the susceptible and partially protected populations over an extended period. This prolonged transmission pressure results in sustained disease spread, leading to a higher number of infected individuals and relatively lower sizes of the susceptible and protected compartments. Conversely, as ξ approaches 1 (integer-order case), the memory effect weakens. The impact of past infections diminishes more rapidly, allowing the prophylactic intervention to act more effectively. The infection chain breaks quickly due to reduced lingering transmission pressure from previously infected cases. As a result, fewer individuals transition into the infected com-

partment, while more individuals remain in or move to the susceptible and prophylaxis-protected compartments. These findings indicate that the fractional-order model with higher ξ values better captures scenarios where prophylactic measures are more successful in controlling Pneumocystis pneumonia transmission within the immunocompromised population.

Figures 6(a), 6(b), and 6(c) show that the transmission rate from unprotected susceptibles to infected individuals (β_1) affects the population dynamics. When β_1 goes up, the sizes of the susceptible and prophylaxis-protected populations shrink while the infected population goes up drastically. The reason for this behavior is that β_1 directly increases the infection term in the model, thereby increasing the force of infection and speeding up the transition of individuals into the infected compartment. The findings here confirm that β_1 plays the primary role in disease spread within the fractional-order framework.

Figures 7(a), 7(b), and 7(c) show how the change in transmission rate from the prophylaxis-protected individuals to the infected ones (β_2) affects the population dynamics. When β_2 increases, the numbers of susceptible and prophylaxis-protected populations both decrease, whereas the infected population increases. The exposed risk increases, so the behavior of prophylactic protection being less effective is reflected here. The parameter β_2, which is the rate of spread of infection from partially protected individuals to susceptible individuals, determines the extent of the protective effect of prophylaxis. As β_2 increases, the impact of the protective measure decreases, while community transmission increases

Figures 8(a), 8(b), and 8(c) show that an increase in the efficacy of the prophylactic drug regimen (ψ) results in a growth of both the susceptible and prophylaxis-protected classes, along with a sharp decrease in the infected class. Formally, an increase in ψ reduces the effective infection term for partially protected individuals, thereby decreasing the total force of infection. From a biological standpoint, it means that enhanced prophylactic effectiveness increases community protection and limits the spread of the disease within the susceptible population.

Figures 9(a), 9(b), and 9(c) depict how the prophylaxis coverage rate for newly at-risk individuals (p) alters population dynamics. As more people are covered, the number of susceptibles decreases, and the number of individuals protected by prophylaxis increases. Moreover, the number of infected people is reduced dramatically. The reason for this change is that more and more newly recruited individuals receive prophylactic protection right away, resulting in fewer unprotected susceptibles and, consequently, a lower overall infection force. On the other hand, the higher the prophylaxis coverage, the better the disease is controlled in the community.

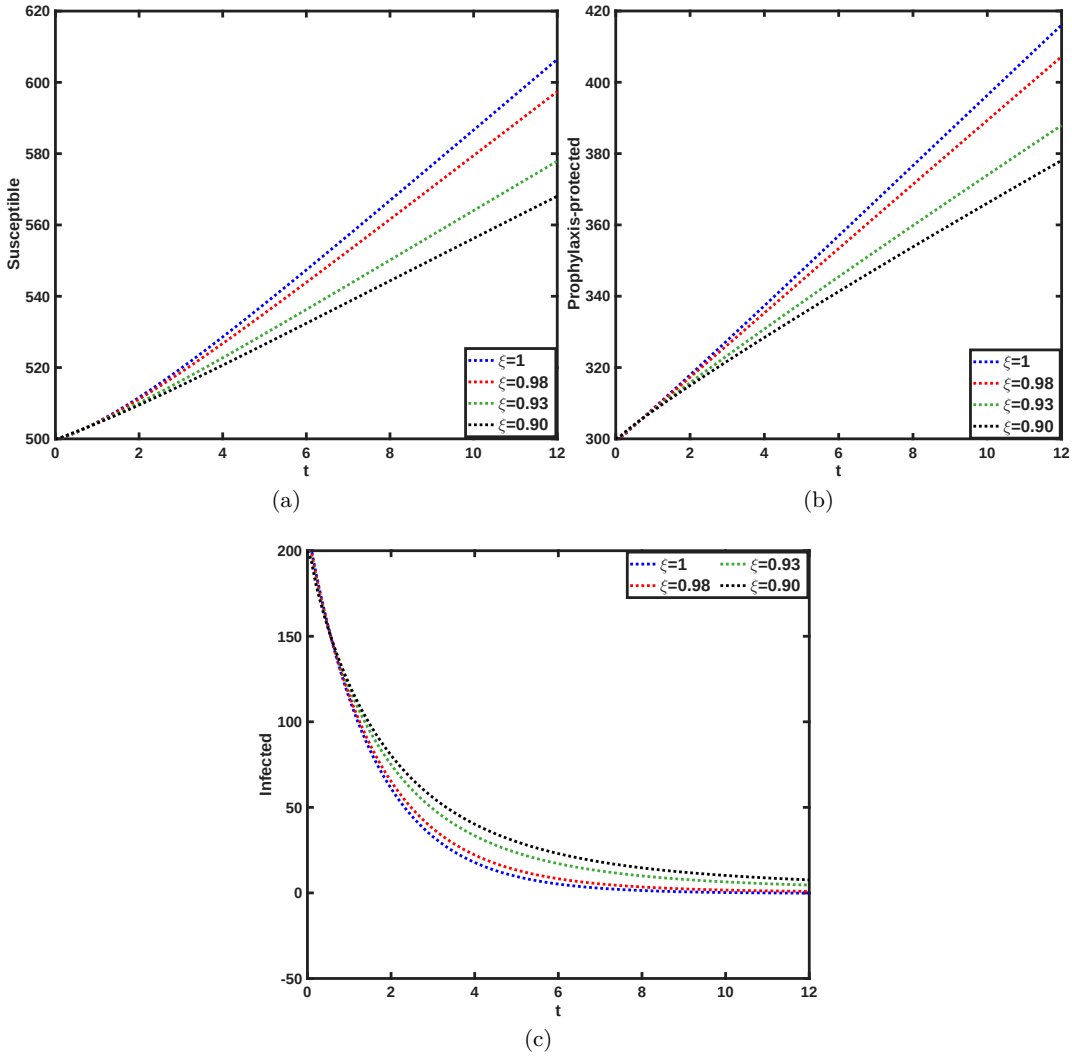

Figure 5: Effect of parameter ξ on population dynamics.

9 Conclusion

In the present study, a novel fractional-order mathematical model based on the Atangana–Baleanu–Caputo derivative was developed to study the transmission dynamics of pneumonia among the immunocompromised population. The model considers prophylactic protection as an imperfect preventive mechanism and, through memory effects in the fractional framework, provides a more realistic representation of disease progression than classical integer-order models. The theoretical analysis has established the positivity, boundedness, existence, and uniqueness

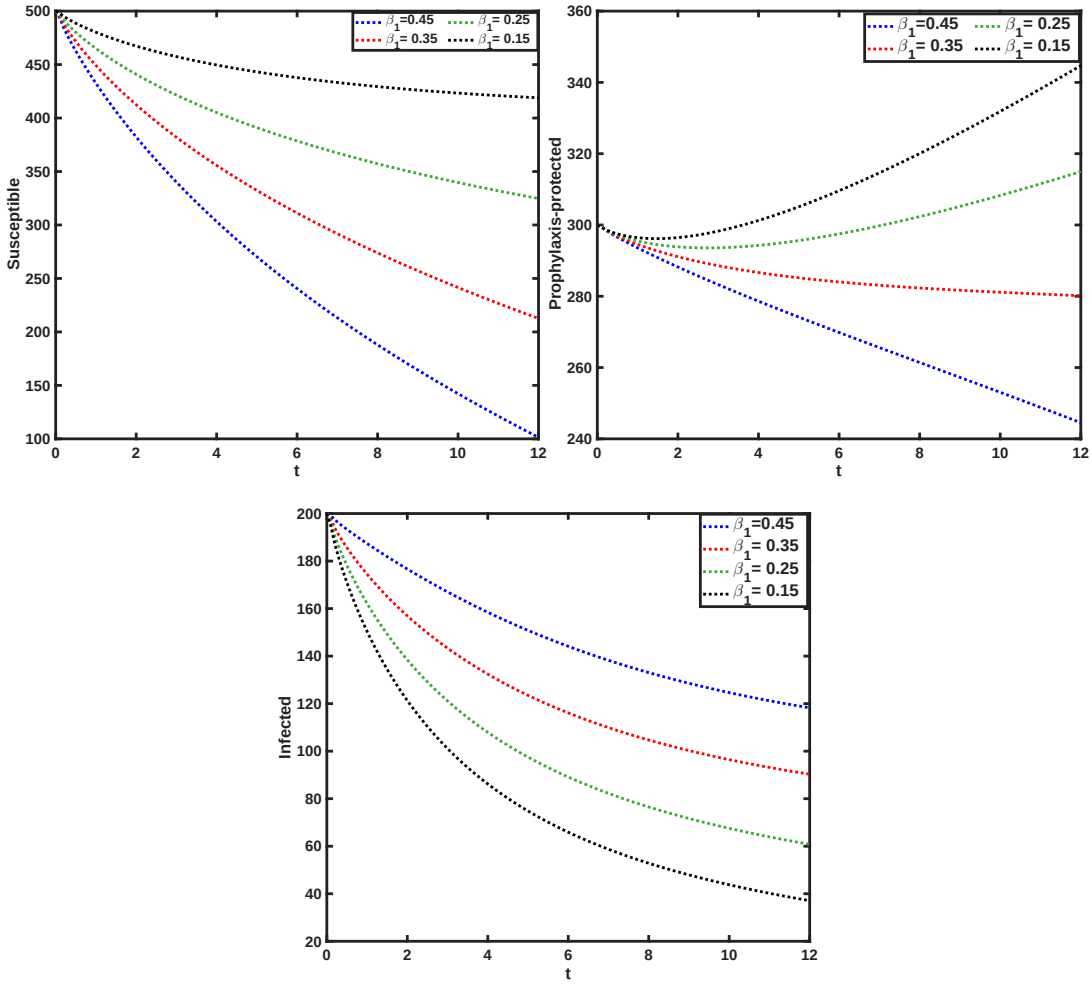

Figure 6: Effect of parameter β_1 on population dynamics.

of solutions, the derivation of the basic reproduction number, and the stability conditions of both the disease-free and endemic EPs. Furthermore, the sensitivity analysis pinpointed the parameters that most significantly affect disease transmission.

Numerical experiments show that high values of transmission rates (β_1 and β_2) result in greater population-wide infection and, subsequently, a more drastic reduction in the number of individuals who remain healthy. Hence, these findings substantiate that contact with infected individuals in the population is the main transmission factor of the disease. However, increases in the efficiency of the prophylactic pharmaceutical drug (ψ) and the fraction of newly infected susceptibles who receive prophylaxis (p) can lead to lower contagion levels and an increase in the

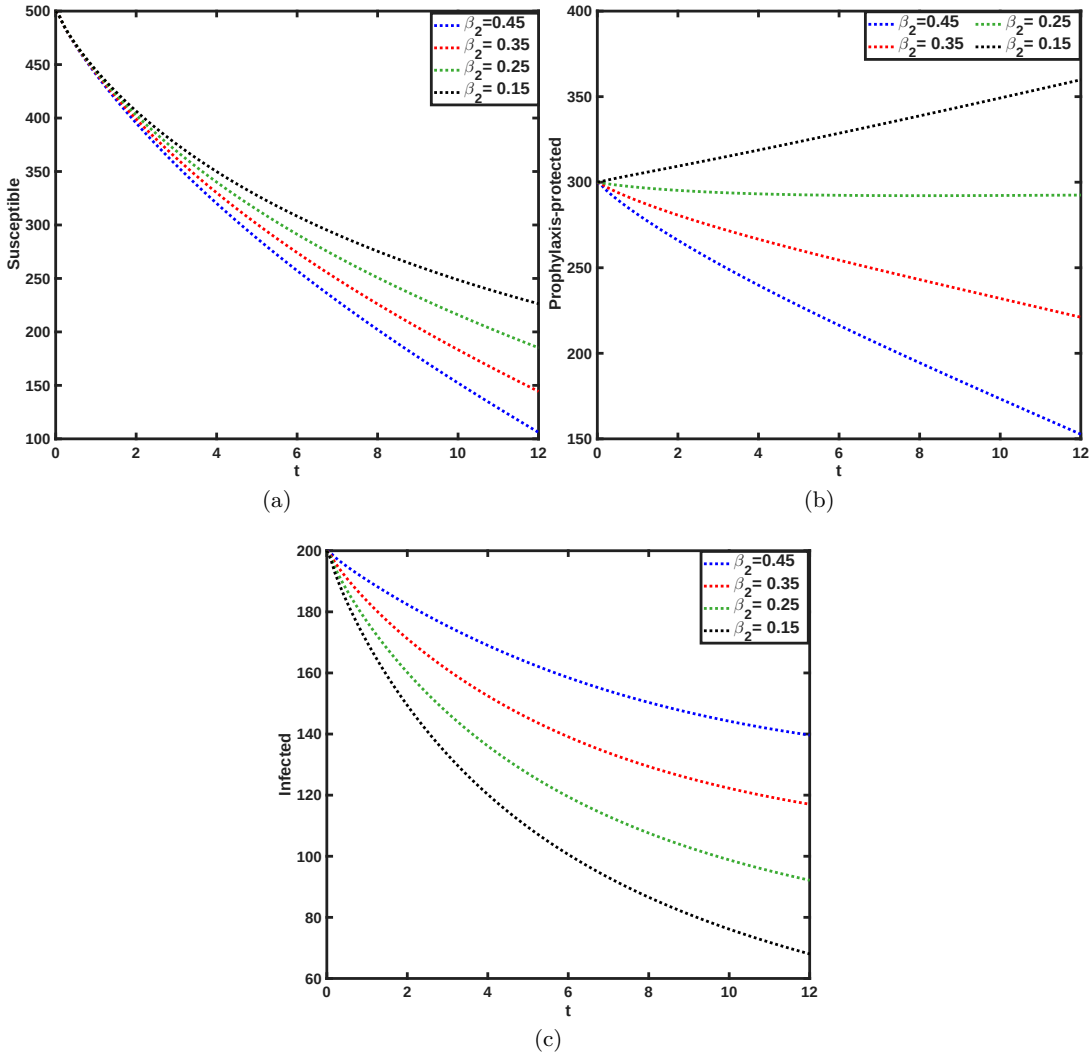

Figure 7: Effect of parameter β_2 on population dynamics.

overall protective power of the population. Moreover, switching to the fractional-order model indicated that the memory effect can influence not only the speed of disease propagation but also the disease pattern in the long run, thereby providing a more complete understanding of changes over time in an epidemic.

The findings of the present study are consistent with previous pneumonia modeling studies [26, 29, 21, 20, 54], which reported that reducing disease transmission and strengthening preventive interventions can significantly limit infection spread. Similarly, the fractional-order pneumonia study in [33] highlighted the important role of the force of infection in disease control.

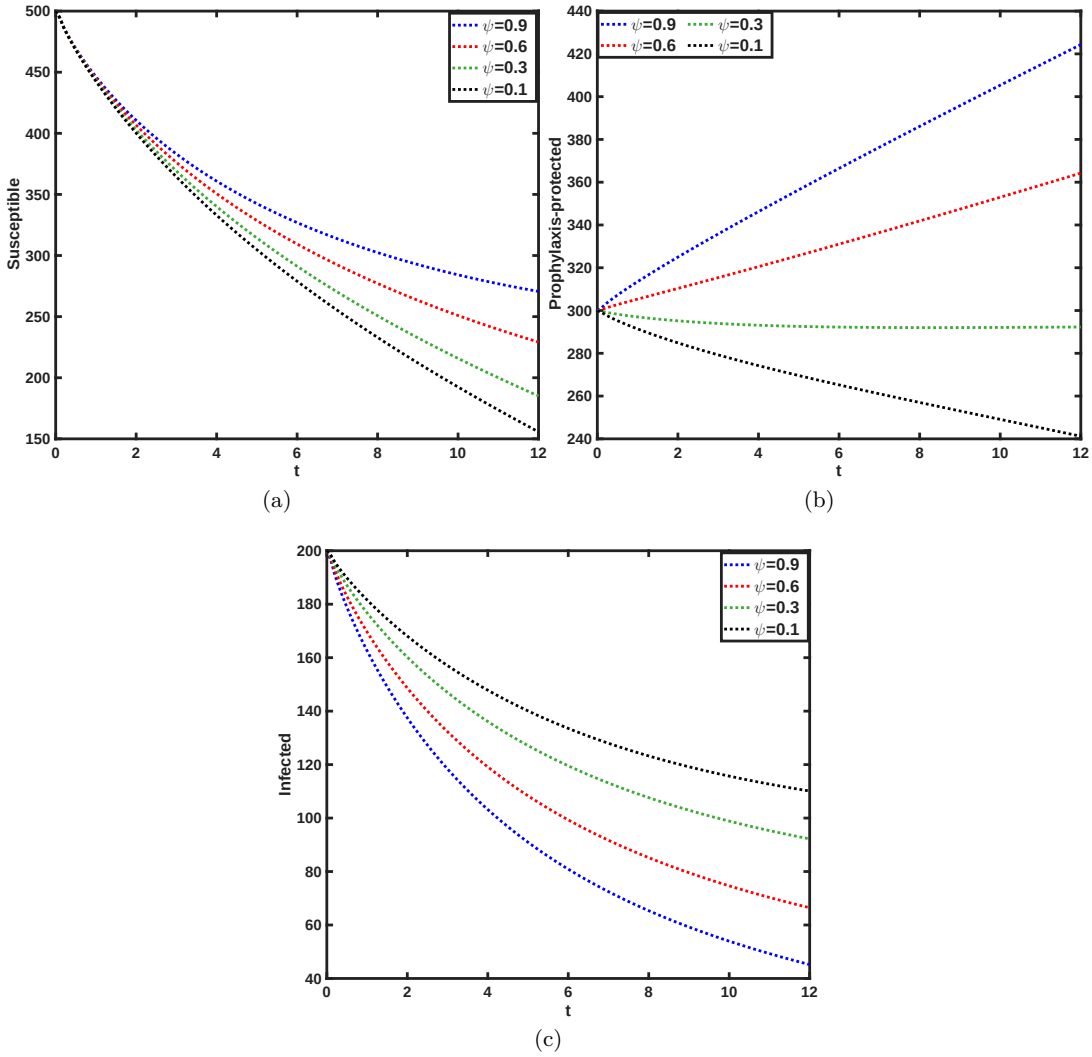

Figure 8: Effect of parameter ψ on population dynamics.

However, unlike these previous studies, the present results specifically demonstrate that increasing prophylaxis coverage and efficacy reduces the infected population in immunocompromised individuals. Moreover, the fractional derivative in the Caputo sense analysis reveals the influence of memory effects on the temporal disease dynamics, providing an additional perspective that is not captured by classical integer-order pneumonia models.

These results, from a health perspective, indicate that to achieve better disease control, a combined approach is necessary that simultaneously reduces transmission, increases the effectiveness of prophylactic drugs, and increases preventive coverage for the most vulnerable groups.

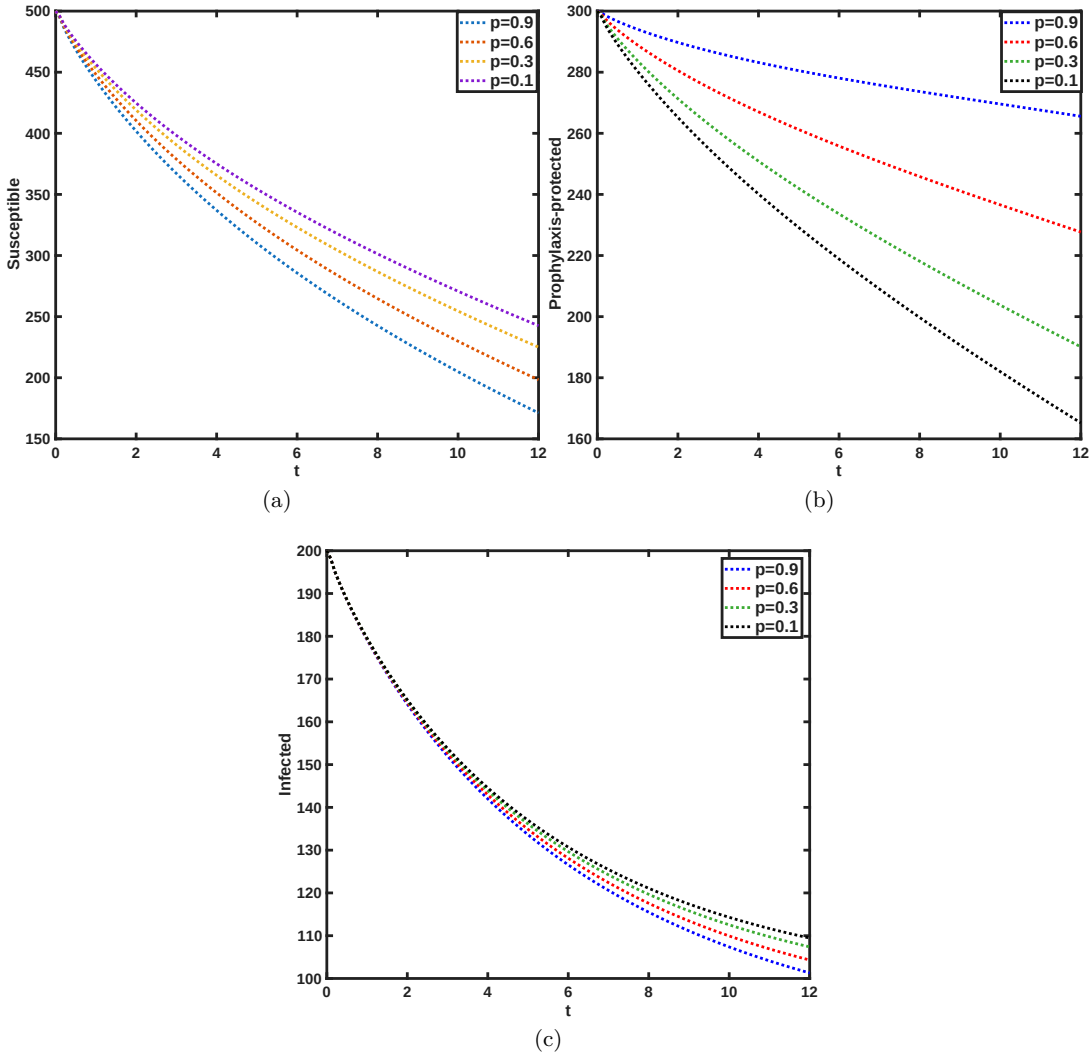

Figure 9: Effect of parameter p on population dynamics.

The study provides measurable grounds for the idea of early intervention through prevention, the use of the most efficient treatment regimens, and behaviour modifications resulting from awareness, which will lead to less contact and, eventually, lower infection rates. Finally, the study lays the groundwork for improved, more precise disease forecasting tools that would then be used to control the spread of infectious diseases among the very vulnerable groups. Additionally, it is a good instrument for public health planning that could be deliberated along with other factors, as it provides one side, the scientific evidence, of the argument. Future work can extend this model by incorporating fear effects, factors, spatial heterogeneity, and co-infection dynamics.

Funding

This research received no external funding.

Conflicts of Interest

The authors declare no conflicts of interest.

References

[1] Almutairi, N. and El-Shahed, M., *Optimal control strategies for a mathematical model of pneumonia infection*, Computation 13(9) (2025) 204.

[2] Alqudah, M.A. and Aljahdaly, N.H., *Global stability and numerical simulation of a mathematical model of stem cells therapy of HIV-1 infection*, J. Comput. Sci. 45 (2020) 101176.

[3] Atangana, A. and Baleanu, D., *New fractional derivatives with nonlocal and non-singular kernel: Theory and application to heat transfer model*, arXiv preprint arXiv:1602.03408 (2016).

[4] Azar, M.M., Cohen, E., Ma, L., Cissé, O.H., Gan, G., Deng, Y., Belfield, K., Asch, W., Grant, M. and Gleeson, S., and Koff, A. *Genetic and epidemiologic analyses of an outbreak of Pneumocystis jirovecii pneumonia among kidney transplant recipients in the United States*, Clin. Infect. Dis. 74(4) (2022) 639–647.

[5] Batiha, I.M., Momani, S., Ouannas, A., Momani, Z. and Hadid, S.B., *Fractional-order COVID-19 pandemic outbreak: Modeling and stability analysis*, Int. J. Biomath. 15(1) (2022) 2150090.

[6] Bhatia, B., Bhatter, S., Purohit, S.D., Baleanu, D. and Suthar, D.L., *A fractional model based on Caputo derivative for tuberculosis transmission using real data from Kenya*, Sci. Rep. 16(1) (2025) 1725.

[7] Bhatia, B., Bhatter, S., Purohit, S.D. and Suthar, D., *Numerical approximation of a time-delayed fractional-order diabetes mellitus model using predictor-corrector method*, Math. Comput. Model. Dyn. Syst. 32(1) (2026) 2658274.

[8] Brown, L., Rautemaa-Richardson, R., Mengoli, C., Alanio, A., Barnes, R.A., Bretagne, S., Chen, S.C., Cordonnier, C., Donnelly, J.P. and Heinz, W.J., and Jones, B. *Polymerase chain reaction on respiratory tract specimens of immunocompromised patients to diagnose Pneumocystis pneumonia: A systematic review and meta-analysis*, Clin. Infect. Dis. 79(1) (2024) 161–168.

[9] Burton, T. and Kirk, C., *A fixed point theorem of Krasnoselskii-Schaefer type*, Math. Nachr. 189(1) (1998) 23–31.

[10] Caputo, M., *Linear models of dissipation whose Q is almost frequency independent–II*, Geophys. J. Int. 13(5) (1967) 529–539.

[11] Caputo, M. and Fabrizio, M., *A new definition of fractional derivative without singular kernel*, Prog. Fract. Differ. Appl. 1(2) (2015) 73–85.

[12] Dunbar, A., Schauwvlieghe, A., Algoe, S., Van Hellemond, J.J., Reynders, M., Vandecasteele, S., Boelens, J., Depuydt, P. and Rijnders, B., *Epidemiology of Pneumocystis jirovecii pneumonia and (non-) use of prophylaxis*, Front. Cell. Infect. Microbiol. 10 (2020) 224.

[13] Ehrhardt, M., Gašper, J. and Kilianová, S., *SIR-based mathematical modeling of infectious diseases with vaccination and waning immunity*, J. Comput. Sci. 37 (2019) 101027.

[14] Gómez-Aguilar, J. and Atangana, A., *Fractional Hunter–Saxton equation involving partial operators with bi-order in Riemann-Liouville and Liouville-Caputo sense*, Eur. Phys. J. Plus 132(2) (2017) 100.

[15] Gómez-Aguilar, J., Torres, L., Yépez-Martínez, H., Baleanu, D., Reyes, J. and Sosa, I., *Fractional Liénard type model of a pipeline within the fractional derivative without singular kernel*, Adv. Differ. Equ. 2016 (2016) 1–13.

[16] Hatzl, S., Posch, F., Scholz, L., Geiger, C., Kriegl, L., Kreuzer, P., Eller, P., Giacobbe, D.R., Bassetti, M., Hoenigl, M., and Krause, R. *Comparative efficacy and safety of treatment regimens for Pneumocystis jirovecii pneumonia in people living with HIV: A systematic review and network meta-analysis of randomized controlled trials*, Clin. Microbiol. Infect. 31(5) (2025) 713–723.

[17] Jain, H. and Sinha, A.K., *Modeling the effect of Wolbachia to control malaria transmission*, Expert Syst. Appl. 221 (2023) 119769.

[18] Jaramillo Cartagena, A., Asowata, O.E., Ng, D. and Babady, N.E., *An overview of the laboratory diagnosis of Pneumocystis jirovecii pneumonia*, J. Clin. Microbiol. 63(3) (2025) e00361–24.

[19] Jin, F., Liang, H., Chen, W.-C., Xie, J. and Wang, H.-L., *Development and validation of tools for predicting the risk of death and ICU admission of non-HIV-infected patients with Pneumocystis jirovecii pneumonia*, Front. Public Health 10 (2022) 972311.

[20] Kanyiri, C.W., Luboobi, L. and Kimathi, M., *Application of optimal control to influenza pneumonia coinfection with antiviral resistance*, Comput. Math. Methods Med. 2020(1) (2020) 5984095.

[21] Kizito, M. and Tumwiine, J., *A mathematical model of treatment and vaccination interventions of pneumococcal pneumonia infection dynamics*, J. Appl. Math. 2018(1) (2018) 2539465.

[22] Kumawat, S., Bhatter, S., Bhatia, B., Purohit, S.D., Baskonus, H.M. and Suthar, D.L., *Novel application of q-HAGTM to analyze Hilfer fractional differential equations in diabetic dynamics*, Math. Comput. Simul. 238 (2025) 136–149.

[23] Kumawat, S., Bhatter, S., Purohit, S.D., Akgül, A. and Hafez, M., *Assessment of brucellosis dynamics through fractional-order models with empirical validation*, Progr. Fract. Differ. Appl. 12(2) (2026) 341–357.

[24] Kushavaha, S.K., Soni, K. and Sinha, A.K., *A fractional-order Zika model with saturated incidence and multiple transmission routes: Analysis and cost-effective optimal control*, Int. J. Dyn. Control 14(188) (2026) 1–34.

[25] Levin, A.S.S., Costa, S., Gobara, S., Caiaffa Filho, H. and Ianhez, L., *A Pneumocystis carinii pneumonia outbreak in a renal transplant unit*, Infect. Control Hosp. Epidemiol. 21(2) (2000) 138–139.

[26] Manuputty, A.H., Lesnussa, Y.A. and Leleury, Z.A., *Stability analysis of pneumonia mathematic model with prevention using vaccines and treatment*, AIP Conf. Proc. 2360 AIP Publishing LLC, 2021.

[27] McDonald, E.G., Afshar, A., Assiri, B., Boyles, T., Hsu, J.M., Khuong, N., Prosty, C., So, M., Sohani, Z.N., Butler-Laporte, G., and Lee, T.C. *Pneumocystis jirovecii pneumonia in people living with HIV: A review*, Clin. Microbiol. Rev. 37(1) (2024) e00101–22.

[28] Odibat, Z.M. and Shawagfeh, N.T., *Generalized Taylor's formula*, Appl. Math. Comput. 186(1) (2007) 286–293.

[29] Ossaiugbo, M.I. and Okposo, N.I., *Mathematical modeling and analysis of pneumonia infection dynamics*, Sci. World J. 16(2) (2021) 73–80.

[30] Peter, O.J., Yusuf, A., Oshinubi, K., Oguntolu, F.A., Lawal, J.O., Abioye, A.I. and Ayoola, T.A., *Fractional order of pneumococcal pneumonia infection model with Caputo–Fabrizio operator*, Results Phys. 29 (2021) 104581.

[31] Reid, A.B., Chen, S.C.-A. and Worth, L.J., *Pneumocystis jirovecii pneumonia in non-HIV-infected patients: New risks and diagnostic tools*, Curr. Opin. Infect. Dis. 24(6) (2011) 534–544.

[32] Saad, K.M. and Gómez-Aguilar, J.F., *Analysis of reaction–diffusion system via a new fractional derivative with non-singular kernel*, Physica A 509 (2018) 703–716.

[33] Saber, S., Alghamdi, A.M., Ahmed, G.A. and Alshehri, K.M., *Mathematical modeling and optimal control of pneumonia disease in sheep and goats in Al-Baha region with cost-effective strategies*, AIMS Math. 7(7) (2022) 12011–12049.

[34] Samko, S.G., *Fractional integrals and derivatives: Theory and applications*, Gordon and Breach, 1993.

[35] Sauvat, L., Denis, L., Nourrisson, C., Poirier, P., Ruivard, M. and Le Guenno, G., *Pneumocystis jirovecii pneumonia in non-HIV patients: Need for a more extended prophylaxis*, Front. Med. 11 (2024) 1414092.

[36] Singh, S.P. and Chandrasekar, P.H., *Pneumocystis jiroveci pneumonia (PJP)*, Medscape (2023). Available at: https://emedicine.medscape.com/article/225976-overview. Accessed: 16 February 2026.

[37] Sinha, A.K. and Soni, K., *Fractional-order modeling of hepatitis B dynamics incorporating socio-environmental factors*, Discov. Public Health 22(1) (2025) 537.

[38] Sinha, A.K., Soni, K. and Purohit, S.D., *A novel fractional mathematical model for the impact of media awareness on hepatitis B*, Math. Open, 5 (2026).

[39] Sintunavarat, W. and Turab, A., *Mathematical analysis of an extended SEIR model of COVID-19 using the ABC-fractional operator*, Math. Comput. Simul. 198 (2022) 65–84.

[40] Solís-Pérez, J., Gómez-Aguilar, J. and Atangana, A., *Novel numerical method for solving variable-order fractional differential equations with power, exponential and Mittag-Leffler laws*, Chaos Solitons Fractals 114 (2018) 175–185.

[41] Soni, K., Kumawat, S. and Sinha, A.K., *Dynamics of Marburg virus in the presence of burial and cremation practices: A fractional approach*, Math. Comput. Sci. 6(3) (2025) 1–22.

[42] Soni, K., Kumawat, S. and Sinha, A.K., *Fractional-order model for Marburg virus transmission: Assessing the impact of awareness, burial and cremation practices*, Beni-Suef Univ. J. Basic Appl. Sci. 14(1) (2025) 109.

[43] Soni, K., Kushavaha, S.K. and Sinha, A.K., *Mathematical model of malaria transmission with prophylactic treatment using Caputo fractional operator*, Frankl. Open (2026) 100688.

[44] Soni, K., Shyamsunder and Sinha, A.K., *Memory-driven dynamics of hepatitis B transmission incorporating media awareness*, Adv. Theory Simul. 9 (2026) e70394.

[45] Soni, K. and Sinha, A.K., *Modeling and stability analysis of the transmission dynamics of monkeypox with control intervention*, Partial Differ. Equ. Appl. Math. 10 (2024) 100730.

[46] Soni, K. and Sinha, A.K., *Modeling Marburg virus control with limited hospital beds: A fractional approach*, Phys. Scr. 100(1) (2024) 015251.

[47] Soni, K. and Sinha, A.K., *Dynamics of epidemic model with conformable fractional derivative*, Nonlinear Sci. 4 (2025) 100040.

[48] Soni, K. and Sinha, A.K., *A novel fractional-order mathematical model for hepatitis B: Impact of awareness*, Int. J. Model. Simul. (2025) 1–18.

[49] Soni, K. and Sinha, A.K., *A fractional-order model for hepatitis B transmission in the framework of nonsingular and nonlocal kernel*, Palest. J. Math. 15(1) (2026) 487–516.

[50] Stavros Anevlavis, M., Kaltsas, K. and Demosthenes Bouros, M., *Prophylaxis for Pneumocystis pneumonia (PCP) in non-HIV infected patients*, Pneumon. 25(4) (2012) 348–350.

[51] Stop Pneumonia / Every Breath Counts, *The forgotten pandemic: 2.5 million annual pneumonia deaths*, (2023). Available at: https://stoppneumonia.org/latest/the-forgotten-pandemic/. Accessed: 16 February 2026.

[52] Syam, M. and Al-Refai, M., *Fractional differential equations with Atangana–Baleanu fractional derivative: Analysis and applications*, Chaos Solitons Fractals X 2 (2019) 100013.

[53] Tasaka, S. and Tokuda, H., *Pneumocystis jirovecii pneumonia in non-HIV-infected patients in the era of novel immunosuppressive therapies*, J. Infect. Chemother. 18(6) (2012) 793–806.

[54] Teklu, S.W., *Investigating the effects of intervention strategies on pneumonia and HIV/AIDS coinfection model*, Biomed. Res. Int. 2023(1) (2023) 5778209.

[55] Teklu, S.W. and Mekonnen, T.T., *HIV/AIDS-pneumonia coinfection model with treatment at each infection stage: Mathematical analysis and numerical simulation*, J. Appl. Math. 2021(1) (2021) 5444605.

[56] Teklu, S.W. and Rao, K.P., *HIV/AIDS-pneumonia codynamics model analysis with vaccination and treatment*, Comput. Math. Methods Med. 2022(1) (2022) 3105734.

[57] UNICEF Data, *Pneumonia*, UNICEF Data: Monitoring the Situation of Children and Women (2023). Available at: https://data.unicef.org/topic/child-health/pneumonia/. Accessed: 16 February 2026.

[58] Xue, T., Kong, X. and Ma, L., *Trends in the epidemiology of Pneumocystis pneumonia in immunocompromised patients without HIV infection*, J. Fungi 9(8) (2023) 812.

[59] Yadav, L., Gour, M., Purohit, S., Al-Mdallal, Q. and Suthar, D., *Generalized Euler method to study the vaccination effects on dynamics of measles infection model under non-singular kernel*, Sci. Rep. 16(1) (2026) 10429.

[60] Yiannakis, E.P. and Boswell, T.C., *Systematic review of outbreaks of Pneumocystis jirovecii pneumonia: Evidence that P. jirovecii is a transmissible organism and the implications for healthcare infection control*, J. Hosp. Infect. 93(1) (2016) 1–8.